Systematics and environmental constrains of earliest brachyurans from the Bajocian, Middle Jurassic, of the north-eastern Iberian Peninsula

FERNANDO A. FERRATGES, BEATRIZ BÁDENAS, MARCOS AURELL, JORGE COLMENAR, and SAMUEL ZAMORA

Ferratges, F.A., Bádenas, B., Aurell, M., Colmenar, J., and Zamora, S., 2026. Systematics and environmental constrains of earliest brachyurans from the Bajocian, Middle Jurassic, of the north-eastern Iberian Peninsula. *Acta Palaeontologica Polonica* 71 (3): 637–659.

The origin of brachyurans or true crabs is elusive. Recent phylogenies and trace fossils point to a Triassic origin, which differs from the fossil record suggesting an Early Jurassic origin. Brachyurans first diversified in the Middle Jurassic in the Tethys, but specimens from such interval are rare and most occurrences are reported from shallow marine oolitic limestones. Here we study the Bajocian (Middle Jurassic) siliceous sponge buildups developed in the proximal deep areas (c. 30–70 m) of a distally-steepened carbonate ramp in the central Iberian Basin (NE Spain), and provide new records of brachyurans from three new localities of the western Tethys. Described taxa include *Iberophthalmus leceraensis* Ferratges & Zamora gen. et sp. nov., ?*Pithonoton* sp., *Tanidromites ciceroides* Ferratges & Zamora sp. nov., *Tanidromites monevaensis* Ferratges & Zamora sp. nov., *Tanidromites* cf. *monevaensis* Ferratges & Zamora sp. nov., and *Tanidromites* cf. *raboeufi*. Although disarticulated, the material is well preserved and includes different anatomical parts suggesting parautochthony of the remains. Sedimentological analysis of the studied successions informs that the Middle Jurassic brachyurans in the western Tethys diversified in shallow marine environments with widespread colonisation of siliceous sponges and later disperse to a wide range of environments including coral and sponge buildups. The described material considerably increases the diversity of brachyurans from the Middle Jurassic supporting the Brachyuran Bajocian Expansion Event (BBEE).

Key words: Brachyura, benthos, siliceous sponge buildups, taxonomy, Bajocian, Jurassic, Spain.

Fernando A. Ferratges [fa.ferratges@igme.es; ORCID: https://orcid.org/0000-0002-9532-6972] and Samuel Zamora [s.zamora@igme.es; ORCID: https://orcid.org/0000-0002-3917-4628], Instituto Geológico y Minero de España, (IGME-CSIC), Campus Aula Dei, Zaragoza 50059, Spain.

Jorge Colmenar [j.colmenar@igme.es; ORCID: https://orcid.org/0000-0002-4323-6975], Instituto Geológico y Minero de España (IGME-CSIC), E-28760, Tres Cantos, Spain.

Marcos Aurell [maurell@unizar.es; ORCID: https://orcid.org/0000-0002-2430-7424] and Beatriz Bádenas [bbadenas@unizar.es; ORCID: https://orcid.org/0000-0003-1112-524X], Departamento de Ciencias de la Tierra-IUCA, Universidad de Zaragoza, Zaragoza 50009, Spain.

Received 14 November 2025, accepted 29 April 2026, published online 24 September 2026.

Introduction

The origin of brachyurans and how they depart from other decapod groups is enigmatic (Krobicki and Zatoń 2008). The oldest brachyurans dated from the Pliensbachian (Early Jurassic) age are *Eocarcinus praecursor* Withers, 1932, from Yorkshire (UK) and *Eoprosopon klugi* Förster, 1986 (Förster 1986; Jagt et al. 2015) from Bavaria (southern Germany). The phylogenetic position of the former has been recently discussed and considered as a stem-group brachyuran (Scholtz 2020). The latter was assigned by Haug and Haug (2014) to the superfamily Homolodromioidea Alcock, 1900.

Although the oldest brachyuran fossils body are Early Jurassic in age (Feldmann and Schweitzer 2010; Tsang et al. 2014), molecular clocks suggest a Triassic origin (Wolfe et al. 2019). The latter is in agreement with trace fossils possibly assignable to brachyurans (Baucon et al. 2025) and

Table 1. Simplified table showing brachyuran taxa from the Middle Jurassic with information on location, environment, and stratigraphy (reference numbers 1–5 indicate the different basins shown in Fig. 1). Abbreviations: N°, number of of specimens; En, facies reference and environment (see legend in Fig. 14); L, lost; *, cast of the holotype.

Taxa	N°	Locality	Basin	En	Stage	References
Abyssophthalmus hebes	2	Moselle Department, France	NE Paris Basin (see 2)	6	lower Bajocian	von Meyer 1840
Abyssophthalmus langrunensis	1	Calvados, France	Paris Basin (see 1)	1	upper Bathonian	Hée 1924
Abyssophthalmus mainense	5	Maine-et-Loire, France	Paris Basin (see 1)	1	lower Callovian	Crônier and Boursicot 2009; Krobicki and Zatoń 2016
Abyssophthalmus bellaii	1	Maine-et-Loire, France	Paris Basin (see 1)	1	lower Callovian	Crônier and Boursicot 2009; Krobicki and Zatoń 2016
?*Abyssophthalmus vilsense*	1	Vilser Alps, Vils, Austria	Vilser Schwelle (Allgäu Basin)	?	lower Callovian	Schweitzer et al. 2007; Van Bakel and Guinot 2023
Bajoprosopon piardi	1	Les Fours à Chaux, France	Paris Basin (see 1)	1	upper Bajocian	Van Bakel et al. 2021
Charassocarcinus mayalis	1	Calvados, France	Paris Basin (see 1)	1	upper Aalenian	Eudes-Deslongchamps, 1877; Van Bakel and Guinot 2023
Coelopus bigoti	L	Vesulien de Falaise, Calvados, France	Paris Basin (see 1)	?	Bathonian	Hée 1924; Schweitzer and Feldmann 2010
Gabriella lugobaensis	1*	Lugoba, N Tanzania	Ruvu Basin	2	?Bajocian/Bathonian	Förster 1985; Schweitzer and Feldmann 2009
Iberophthalmus leceraensis gen. et sp. nov.	2	Lécera, Spain	Iberian Basin	4	upper Bajocian	this paper
Meroncarcinus boursicoti	1	Calvados, Méron, near Montreuil-Bellay, Maine-et-Loire, France	Paris Basin (see 1)	1	Callovian	Van Bakel and Guinot 2023
Nodoprosopon sp.	1	Kraków, Poland	Polish Basin (see 3)	6	lower Callovian	Krobicki and Zatoń 2008
Pithonoton incisum	1	Calvados, France	Paris Basin (see 1)	2	upper Bajocian	Van Straelen 1925; Feldmann et al. 2006
Pithonoton moutieri	1	Moult, Calvados, France	Paris Basin (see 1)	2	upper Bathonian	Hée 1924; Wehner 1988
Pithonoton sp.	1	Czerwieniec, Kraków region, S Poland	Polish Basin (see 3)	6	lower Callovian	Krobicki and Zatoń 2008
Planoprosopon major	1	May-sur-Orne, Calvados, France	Paris Basin (see 1)	2	?upper Bajocian	Hée 1924
Planoprosopon quadratum	?	NE Germany	North German Basin/ Sub-boreal epicontinental sea	?	middle Callovian	Schweigert and Koppka 2011
Prosopon mammillatum	3	Stonesfield, Oxfordshire, England, UK	Eastern Oxfordshire Basin	1	middle Bathonian	Woodward 1868; Wehner 1988
Prosopon sp.	1	Lugoba, N Tanzania	Ruvu Basin	2	?Bajocian/Bathonian	Förster 1985
Protocarcinus auduini	?5	Langrune, Ranville, Calvados, France	Paris Basin (see 1)	2	Bathonian	Eudes-Deslongchamps 1835; Schweitzer and Feldmann 2009
Tanidromites maerteni	1	Maizet (Calvados)	Paris Basin (see 1)	1	lower Bajocian	Fraaije et al. 2013
Tanidromites montreuilense	3	Maine-et-Loire, France	Paris Basin (see 1)	1 or 5?	lower Callovian	Crônier and Boursicot 2009
Tanidromites lithuanicus	1	Popilani, Papartinė near Papilė, northern Lithuania	E Polish Basin? (see 4)	6	middle Callovian	Schweigert and Koppka 2011
Tanidromites muelleri	46	Kawodrza Górna, near Czestochowa, central Poland	Polish Basin	5	upper Bajocian	Krobicki and Zatoń 2016
Tanidromites richardsoni	?1	Somerset and Cotswolds, England, UK	Southern England epicontinental sea	1	upper Bajocian	Withers 1951; Schweigert and Koppka 2011; Van Bakel et al. 2021
Tanidromites raboeufi	?	La Bigotière, Crannes-en-Champagne, France	Paris Basin (see 1)	5	upper Bathonian	Robin et al. 2015
Tanidromites ciceroides Ferratges & Zamora sp. nov.	16	Moneva, Lécera, Spain	Iberian Basin	4	lower–upper Bajocian	this paper
Tanidromites monevaensis Ferratges & Zamora sp. nov.	46	Moneva, Spain	Iberian Basin	4	lower–upper Bajocian	this paper
Tanidromites cf. *monevaensis* Ferratges & Zamora sp. nov.	3	Lécera, Spain	Iberian Basin	4	lower Bajocian	herein
Tanidromites cf. *raboeufi*	1	Moscardon, Spain	Iberian Basin	4	upper Bajocian	herein
Tanidromites sp.	1	Moneva, Spain	Iberian Basin	4	lower–upper Bajocian	herein
Verrucarcinus marsae	3	Calvados and Maine-et-Loire, Saint-Laon quarry, Vienne Department, France	Paris Basin (see 1)	1	Callovian	Van Bakel and Guinot 2023
Vilsercarcinus keuppi	1	Germany, Austria	Vilser Schwelle (Allgäu Basin) (see 5)	1	upper Toarcian–Callovian	Van Bakel and Guinot 2023

Fig. 1. Middle Jurassic palaeogeography of part the northern hemisphere indicating the location of the basins including the known brachyurans fossil sites listed in Table 1 (modified from Aurell and Bádenas 2015). Palaeogeographic map of Europe at 175 Ma based on Blakey (2021). The depositional area of the "Vilser Schwelle" is located within the Austroalpine nappes (southern margin of the Tethys Ocean) and cannot be accurately represented on this map.

the occurrence of microcoprolites of brachyurans or their Triassic ancestors (Schweigert et al. 1997).

The homolodromoid crabs, a controversial group of earliest brachyurans, have been considered as ancestral to all other brachyurans (i.e., Krobicki and Zatoń 2008; Tsang et al. 2014; Davie et al. 2015; Wolfe et al. 2021) and they were the dominant group in the Jurassic (Table 1).

The earliest homolodromoids from the Middle Jurassic lived both in shallow warm waters with organic buildups, and on muddy siliciclastic environments (Krobicki and Zatoń 2008; Crônier and Boursicot 2009). Just after their origin, the first diversification pulse of brachyurans occurred in the Bajocian (Middle Jurassic) in the so-called Brachyuran Bajocian Expansion Event (see Krobicki and Zatoń 2016; Van Bakel et al. 2021). Most records of Bajocian homolodromoids come from localities that were part of epicontinental seas adjacent to the northwestern Tethys Ocean (Krobicki and Zatoń 2016) like France, England, Germany, and Poland (Schweigert and Koppka 2011; Van Bakel et al. 2021) (Fig. 1).

Krobicki and Zatoń (2008: fig. 8) suggested that early habitats for homolodromoids were closely related to oolitic, crinoidal and coral facies, as well as molluscan buildups or shell accumulations. Furthermore, the homolodromoids inhabited moderately deep-water grey clayey facies, while only later invading sponge facies. The problem is that the record of earliest brachyurans is extremely patchy and most taxa are described based on just one specimen (Table 1). This is exacerbated by the fact that taphonomic and sedimentological information from almost all these occurrences is lacking (see exception in Krobicki and Zatoń 2008), hampering our ability to understand the habitats that the earliest brachyurans occupied.

In order to understand the distribution of early brachyurans in the western Tethys, we have selected several outcrops of Middle Jurassic rocks located in the central part of the Iberian Chain (NE Spain). Homolodromoids in this area are at least present in the Upper Jurassic outcrops (Via and Sequeiros 1989) but have never been reported in older rocks. The Bajocian (Middle Jurassic) outcrops of the Iberian Chain show a mosaic of facies with local development of siliceous sponge buildups, including from small patches to big mounds. Detailed sedimentological studies in the two key localities of Ricla (Bersán and Aurell 1997; Tomás et al. 2019) and Moscardón (Aurell and Bádenas 2015) reveals that buildups developed in relatively proximal deep carbonate ramp areas located close to the storm wave base.

The aims of this work are: (i) describe new localities with the earliest brachyurans from Iberia; (ii) discuss the palaeoenvironmental constrains of these occurrences based on sedimentological data; (iii) describe new forms of homolodromoids from Spain; (iv) treat such occurrences in a global context and discuss possible bias in the origin of earliest brachyurans. The rocks of these study sites are uppermost lower Bajocian (*Stephanoceras humphriesianum* Ammonite Zone), and the upper Bajocian (*Garantiana garantiana*, *Strenoceras niortense*, and *Parkinsonia parkinsoni* ammonite zones), therefore offering a good opportunity for deciphering the diversification of decapod crustaceans of Bajocian age.

Institutional abbreviations.—MPZ, Museo de Ciencias Naturales de la Universidad de Zaragoza, Spain.

Other abbreviations.—BOEE, Brachyuran Oxfordian Explosion Event; BPOE, Brachyuran Pliensbachian Origin Event; CL, carapace length; CW, carapace width.

Nomenclatural acts.—This published work and the nomenclatural acts it contains have been registered in ZooBank: urn:lsid:zoobank.org:pub:F66A5ECA-E288-4192-B78A-161411156C75.

Geological setting

The Bajocian (Middle Jurassic) outcrops that include the studied fossil sites are located in the central part of the Iberian Chain in the northeast of the Iberian Peninsula (Fig. 2A). These ranges formed after the latest Cretaceous–earliest Neogene compressional tectonic inversion of the Iberian Basin rift system. Previous to this inversion, this rifting basin evolved during different stages of Mesozoic extension related to the opening of the Alpine Tethys and the Atlantic (e.g., Aurell et al. 2019, 2022; Martín-Chivelet et al. 2019).

During the Middle Jurassic, the central and eastern Iberian Basin was characterised by the presence of two NW-SE-trending open marine platform areas, delimited by shallow marine and low-subsidence zones (Fig. 2B). This palaeogeographic distribution was related to extensional tectonics, primarily controlled by the final rifting phase that preceded the opening of the oceanic Alpine Tethys (Gómez and Fernández-López 2006; Aurell et al. 2019). The Bajocian sedimentary record in this basin includes two third-order transgressive-regressive sequences (T-R sequences Baj-1 and Baj-2 in Fig. 2C) linked to regional sea-level changes with possible influence of the global eustacy (Aurell et al. 2003). The stratigraphic succession that includes the studied fossil sites spans the upper part of the Baj-1 Sequence and the Baj-2 Sequence (Fig. 2C), both belonging to the Chelva Group (Gómez and Fernández-López 2006).

The studied fossil sites originated in certain sedimentary domains of the open platform areas characterised by the common occurrence of siliceous sponge-microbial facies (dark blue areas in Fig. 2B). In these domains, sponge-microbial buildups of variable size (from small patches to big mounds) have been described in detail (Friebe 1995; Bersán and Aurell 1997; Aurell and Bádenas 2015; Tomás et al. 2019). Most of these buildups developed at the end of the early Bajocian (*S. humphriesianum* Ammonite Zone) and during the late Bajocian. The taxonomic composition of siliceous sponges in these buildups is variable. In large areas of the Iberian Basin, the lower Bajocian buildups are dominated by hexactinellid sponges, whereas lithistid sponges became more abundant in the upper Bajocian successions (Friebe 1995).

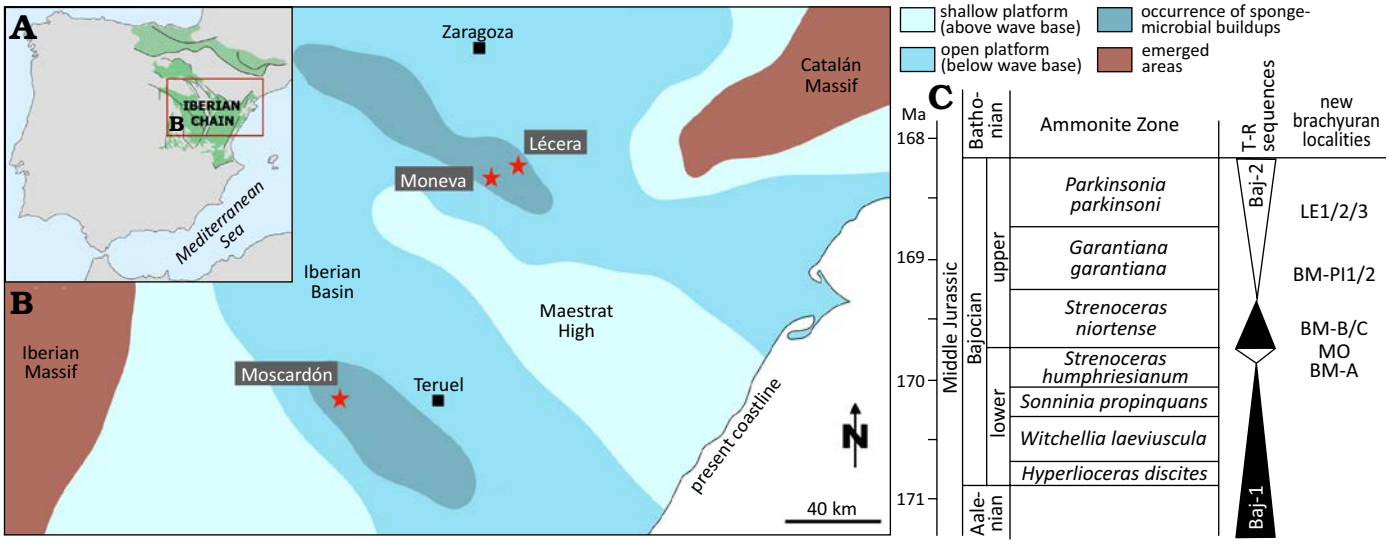

Fig. 2. **A**. Location of Iberian Chain in northeastern Spain. **B**. Palaeogeography of the Iberian Basin during the Bajocian, indicating the localities studied in the present work (stars) (modified from Aurell and Bádenas 2015). **C**. Chronostratigraphic location of the studied brachyurans fossil sites in the Iberian Basin, based on ammonite biostratigraphy. Third-order transgressive-regressive sequences (T-R sequences Baj-1 and Baj-2) are also indicated. MO, Moscardón fossil site; BM-A, BM-B, BM-C, BM-PI1, and BM-PI2, Moneva fossil sites; LE1 to LE-3, Lécera fossil sites.

Sponge and coral buildups including a variable proportion of microbialites grew not only in the Iberian Basin, but also in certain open marine domains of the Jurassic carbonate platforms that developed along the western Tethys (Leinfelder and Schmid 2000). Coral-microbial reefs occurred in shallow platform areas with moderately oligotrophic to mesotrophic conditions, whereas microbial-siliceous sponge buildups grew in relatively deep marine domains, from extremely oligotrophic to strongly mesotrophic settings. Furthermore, periods of high nutrient concentrations could have been responsible for the development of microbialites and siliceous sponges on the Jurassic platforms, and therefore, detrimental to coral growth (e.g., Leinfelder et al. 1993; Dupraz and Strasser 2002; Olivier et al. 2006, 2008; Aurell and Bádenas 2015).

Material and methods

Studied sections and facies analysis.—Three key stratigraphic sections, Moscardón (~70 m thick), Moneva (~50 m thick), and Lécera (~35 m thick), have been selected for stratigraphic-sedimentological analysis of the Bajocian successions in order to situate the different levels bearing brachyurans and locate the intervals including microbial-sponge buildups. Stratigraphy and sedimentological analysis of the Moscardón outcrop was already performed in Aurell and Bádenas (2015), so only a summary of main features is included here. The Moneva and Lécera sections have been studied in detail for the present work. This study has included a bed-by-bed logging of geometry, lithology, texture, components and sedimentary structures of the strata, sampling of ammonite fossils for biostratigraphic dating (10 sites in Moneva; 4 sites in Lécera) and rock sampling for study of thin-sections under petrographic microscope for facies determination (a total of 40 thin sections). The combination of data for field/laboratory study of facies and analysis of field photographs allowed the identification of the location of brachyurans fossil sites in relation to the microbial-sponge buildups.

Brachyurans sampling and preparation.—Jurassic localities bearing sponge facies have been sampled for decapod crustaceans. They include most of the areas described by Fernández López (1985) and Friebe (1995). Other Middle Jurassic successions have been also explored for comparison by the authors, but without positive results. The three studied sections have been extensively explored for decapod crustaceans. Nine fossil levels bearing well-preserved brachyurans have been recognised and extensively sampled: one fossil level in Moscardón (MO site); five levels in Movera (BM-A, BM-B, BM-C, BM-PI1, and BM-PI2 sites); and three levels in Lécera (LE-1 to LE-3 sites). These levels correspond to the uppermost lower Bajocian (*S. humphriesianum* Ammonite Zone) and the upper Bajocian *G. garantiana*, *S. niortense*, and *P. parkinsoni* ammonite zones (Fig. 2C).

The studied localities have been systematically prospected by fragmenting rocks collected in situ from different areas and stratigraphic levels of the outcrops and examining the rock surfaces using hand lens. When fossil-bearing areas were identified, intensive sampling was carried out with the aim of obtaining the maximum number of specimens. The rock blocks have been fragmented to a size of a few centimetres (between 1 and 5 cm) during 4–5-hour sessions, carried out by groups of 2–3 people over a total of 15 non-consecutive days. Rocks have been extracted and fragmented and all decapod remains have been taken to the laboratory for further microscopic analysis. Specimens are relatively small (ca. 1 cm or less) and have been prepared using a Micro Jack 2 air scribe (Paleotools) with the help of a needle under a ×40 binocular magnifying glass. Both internal and external moulds have been mechanically prepared. The latter have been also casted using latex which allows observation of anatomical details from the external part of the carapaces. Specimens were deposited in the Museo de Ciencias Naturales de la Universidad de Zaragoza under the acronym MPZ.

Analysis of diversity.—A brachyurans diversity curve was calculated using all known global occurrences gathered from the bibliography (see SOM 1, Supplementary Online Material available at http://app.pan.pl/SOM/app71-Ferratges_etal_SOM.pdf), plus adding the new data from the Iberian Basin presented here (Table 1). Taxa occurrences with unknown palaeoenvironmental information have been discarded from the analyses. A list of taxa excluded from the analysis and the reason for their exclusion can be found in SOM 1. The occurrences have been divided into time bins; in this case the Jurassic substages shown in Ogg et al. (2016) that are well-constrained by ammonite biozonation, have been selected. For constructing the cumulative diversity curve, the number of different species present in each time bin have been counted. From each taxon, the complete stratigraphic range has been considered, i.e., if a specific taxon occurs in the Lower Jurassic, does not occur the Middle Jurassic, but occurs again in the Upper Jurassic, it will be counted in the Middle Jurassic as well, since it should have been present in that time bin but was not recorded for any reason (e.g., sampling artifact).

Additionally, the palaeonvironmental information of each occurrence (Table 1) has been also added in the curve, showing the preferences of the taxa for each particular environment in each time bin.

Stratigraphy and palaeoenvironmental reconstruction

The main stratigraphical and sedimentological features of the Bajocian successions including the brachyuran fossil sites, Moscardón, Moneva, and Lécera, are provided in the synthetic logs (Figs. 3 and 4, respectively). A detailed description of the main facies drawn in these logs is offered

Table 2. Detailed description of the main facies recorded in the Bajocian successions in the studied Moscardón (Fig. 3), Moneva and Lécera sections (Fig. 4). See also Figure 5 for palaeoenvironmental interpretation of facies.

Facies	Texture and components	Stratification and sedimentary structures	Sub-environment
Intraclastic-bioclastic-peloidal packstones-grainstones (locally microbial encrusted)	Grain-supported coarse to fine-grained facies with variable proportions of: – cm-thick fragments of sponges and echinoderms (echinoids, crinoids) – submillimetre-sized peloids to millimetre-sized intraclasts (micritic, fragments of microbial crusts) – fine bioclasts: sponge spicules, echinoderms, bivalves, gastropods, benthic foraminifera (nubeculariids, *Dentalina*, *Nodosaria*, *Trocholina*), serpulids – mm-sized coated intraclasts/micritic ooids	– tabular dm- to m-thick beds – microbial-encrusted intervals concentrated at the base and top of the beds	shallow ramp
Microbial-sponge buildups (patches)	Boundstones formed by: – Hexactinellida and Lithistida siliceous (calcified) sponges with cup and tube morphologies – microbial crusts: irregular interlamination of dense (i.e., massive) and clotted (i.e., micropeloidal) crusts, with domal morphologies and laminated fabrics, with microencrusters (worm tubes, *Terebella*), encrusting foraminífera (nubeculariids) and bryozoans – mm-width cavities (intergrowth cavities, borings, stromatactis-like cavities) filled with muddy to micropeloidal-bioclastic internal sediment (echinoderms, bivalves, brachiopods, foraminifera, sponge spicules, serpulids) – Lithistida sponges dominate within the patches; colonial corals in growth position are also present	– 1 m-thick, few m-width – concave-convex and inverted-cone shape	proximal deep ramp
Microbial-sponge buildups (mounds)		– vertically-stacked tabular biostromes, forming lenses/mounds up to 35 m thick and 50–100 m wide – outcrops in Moscardón reveal mounds are asymmetric showing up-dip flanks with dips of a few degrees and down-dip flank dipping up to c. 25°	distal deep ramp
Sponge limestones (floatstones to rudstones), marly limestones and marls	Muddy facies including from marls to marly limestone and limestones. Marly limestones and limestones have variable proportions of: – Hexactinellida and Lithistida siliceous (calcified) sponges with cup and tube morphologies both in growth position and slightly reworked, forming floatstones to rudstones textures – fine-grained matrix (from wackestone to packstone texture) including sub-millimetre sized peloids to mm-sized intraclasts (fragments of microbial crusts) and fine poorly-rounded bioclasts: echinoderms, bivalves, brachiopods, gastropods, benthic foraminifera, bryozoans; occasionally thin-shelled *Bositra*-like are abundant – entire ammonites, bivalves and brachiopods are frequent; belemnites are also present	– tabular dm-thick beds, locally arranged in m-thick packages – usual bioturbation and ferruginous top surfaces – local depositional inclination reflects hardening/cementation with probably microbial mediation	proximal to distal deep ramp
Bivalve (*Bositra*-like) packstones	– fine bioclasts dominated by *Bositra*-like bivalves, also debris of echinoderms, other bivalves, brachiopods, gastropods, sponge spicules, serpulids, benthic foraminifera, ammonites – local intraclasts (fragments of microbial crusts) and debris of encrusted sponges – micropeloidal matrix and usual glauconite grains	– tabular dm-thick beds – usual bioturbation	distal deep ramp

in Table 2. The sedimentological interpretation of facies/subenvironments within the platform and the palaeoenvironmental location of the fossil sites is included in Fig. 5. Main features are summarised below.

Moscardón.—Aurell and Bádenas (2015) reconstructed the stratigraphic architecture, including facies and sequences, of the Bajocian of Moscardón in the c. 1 km-long down-dip platform transect exposed in a continuous outcrop. Age constrains of the two Bajocian T-R sequences (Baj-1 and Baj-2, Fig. 2C) characterised in this transect are based in the ammonite biostratigraphy provided by Fernández-López (1985). In the zone of the Moscardón outcrop that includes the MO fossil site, the Baj-1 sequence is dominated by a large (more than 35 m-thick) microbial-sponge buildup (Fig. 3A). This buildup shows a significant inclination (c. 25°) in its northern (down dip) flank. However, the southern (more proximal) flank is nearly horizontal. The overall reconstruction of the Moscardón outcrop shows that this large buildup grew in the proximal deep ramp, below wave (storm) base, at a depositional depth ranging around 50–70 m (Fig. 3B). The observed vertical accretion (aggradation) and lateral growth (progradation) of the Moscardón buildup (Fig. 3A) was related to changes in accommodation space in accordance to the transgressive and regressive hemicycles of the Baj-1 sequence, respectively (Aurell and Bádenas 2015). The overlying Baj-2 sequence has also a deepening-shallowing facies evolution, and in the uppermost part consists of well-cemented intraclastic-bioclastic-peloidal packstones-grainstones deposited above wave base (Figs. 3 and 5).

The MO fossil site (coordinates: 40°20’00.6”N 1°32’23.7”W) is located in the lowermost levels of the regressive hemicycle of Baj-1 sequence, in the upper *S. humphriesianum* Ammonite Zone. Brachyurans include only the species of *Tanidromites* cf. *monevaensis* Ferratges & Zamora sp. nov. and were preserved in sponge limestones, marly limestones, and marls forming the down-dip flank and bottom sediments of the Baj-1 sequence mound. The predominantly muddy texture and variable proportion of sponges and other skeletal components (Table 1) is coherent with deposition below wave base and preservation of high angle of depositional inclination reflects rapid lithification of the sediments probably related to microbial activity (Aurell and Bádenas 2015). These observations allow us to locate the MO site in the low-energy muddy sediments of the down-dip side of a microbial-sponge mound (Fig. 5).

Moneva.—The outcrop of Moneva includes five fossil sites (BM-A, BM-B, BM-C, BM-PI1, and BM-PI2; coordinates: 41°07’02.5”N 0°48’02.1”) located at different stratigraphic

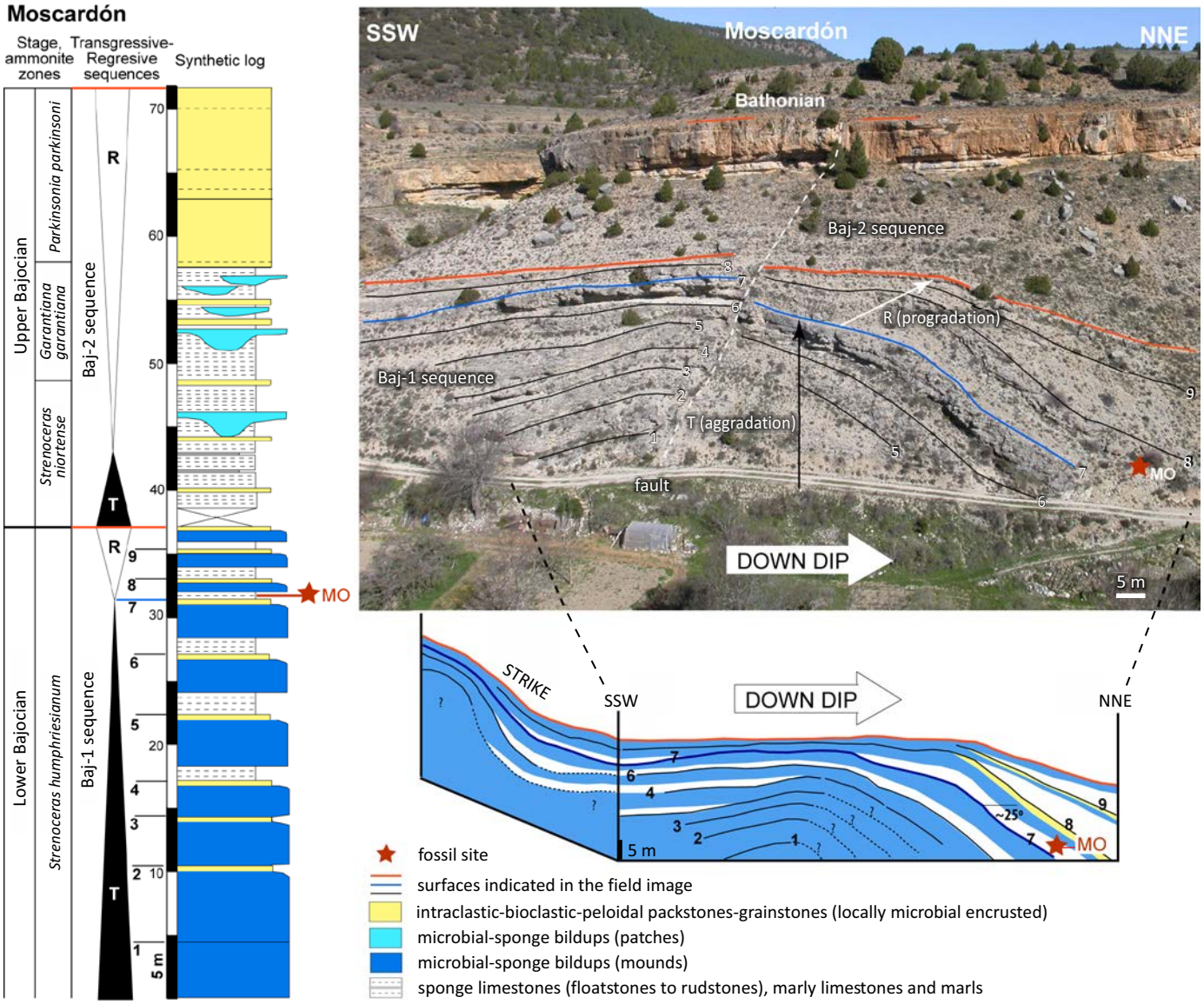

Fig. 3. Synthetic stratigraphic-sedimentological log of the Bajocian succession in Moscardón, and field images and sketch indicating the location of MO fossil level in the muddy facies at the down-dip flank of a large microbial-sponge buildup developed in the *S. humphriesianum* Zone, within the regressive hemicycle of the Baj-1 sequence. MO coordinates: 40°20'00.6"N 1°32'23.7"W.

levels (Fig. 4). New ammonite and facies analyses reported here allowed the characterisation of the two Bajocian depositional sequences, Baj-1 and Baj-2. The lower Bajocian Baj-1 sequence is highly condensed at its lower part. This condensed interval corresponds to a ~3 m-thick succession of limestones dominated by *Bositra*-like packstones, with local iron ooids and glauconite that includes in its upper part ammonites of the *S. propinquans–O. sauzei* Zone (Bulard 1972). Above this interval, ammonites of the *S. humphriesianum* Zone have been collected in successive levels of the sequence. As a whole, the Baj-1 sequence consists of a ~17 m-thick succession including large microbial-sponge mounds, showing an aggradational-progradational stacking (i.e., transgressive-regressive), similar to what is observed in the age-equivalent succession of Moscardón. Deposition of discrete beds of shallow-water intraclastic-bioclastic-peloidal facies coeval with the progradational stacking of the mound points to the regressive tendency at the upper part of the sequence. The BM-A fossil site is located in the transgressive hemicycle of the sequence in the middle part of the *S. humphriesianum* Zone, therefore older than MO site in Moscardón (Figs. 2C and 3). BM-A consists of the muddy sediments (sponge limestones, marly limestones, and marls) lateral to these large buildups, in similar facies to MO site in Moscardón (Fig. 5). Species at this site include *Tanidromites ciceroides* Ferratges & Zamora sp. nov.

The Baj-2 sequence is ~31 m-thick and has a clear transgressive-regressive facies trend including a lower transgressive hemicycle dominated by muddy facies (sponge-rich limestones, marly limestones, and marls) and an upper regressive hemicycle encompassing muddy facies with intercalated small microbial-sponge patches less than 1 m-thick

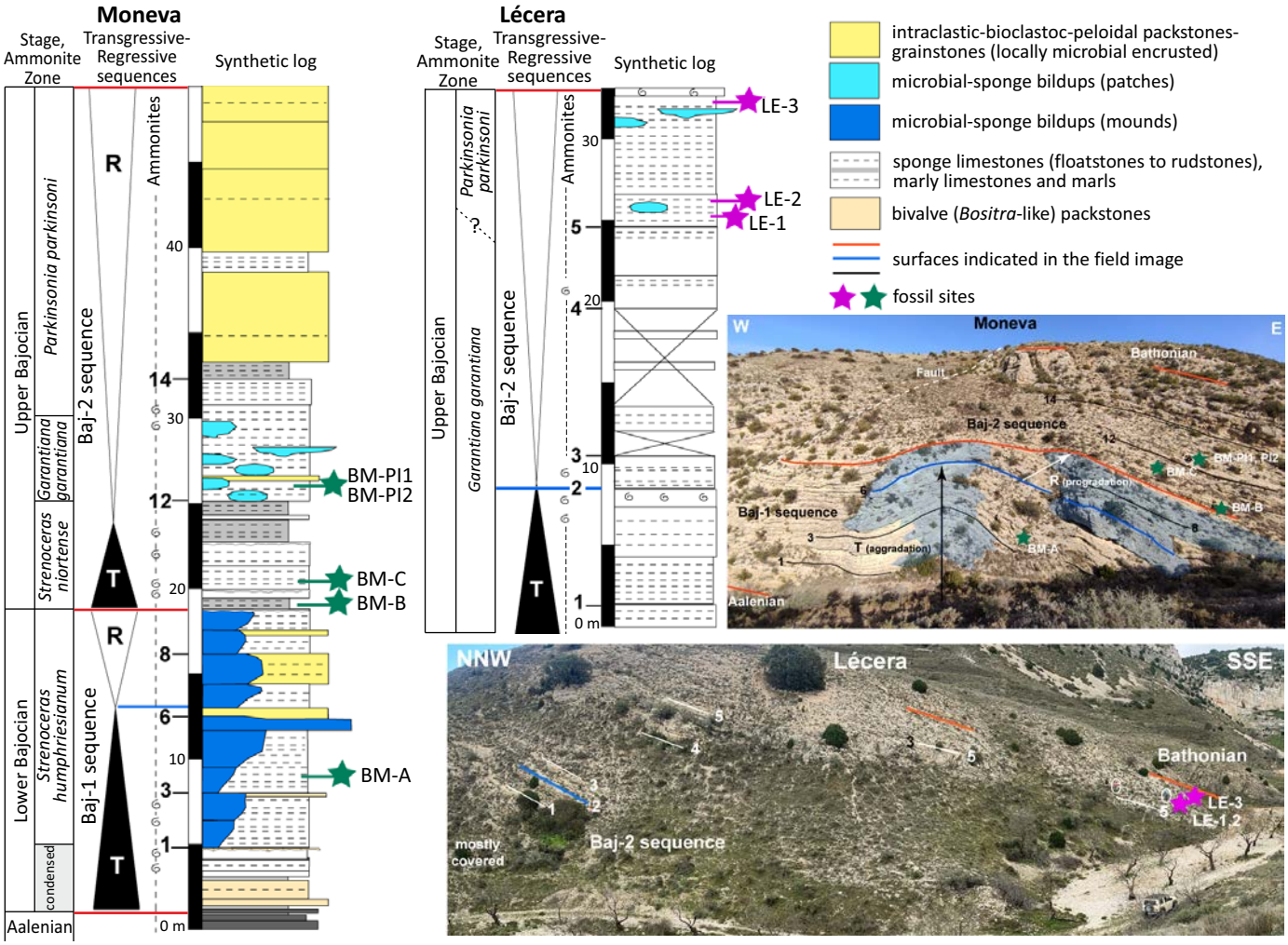

Fig. 4. Synthetic stratigraphic-sedimentological logs and field images of the Bajocian successions in Moneva and Lécera, indicating the location of Moneva fossil levels (BM) and Lécera fossil levels (LE) in the muddy facies related to microbial-siliceous mounds and patches. BM-A locates in the transgressive hemicycle of the Baj-1 sequence, therefore older than the Moscardón fossil site MO. The rest of levels are upper Bajocian in age encompassing the three ammonite zones of the upper Bajocian. Coordinates: 41°07'02.5"N 0°48'02.1" (BM); and 41°09'33.6"N 0°44'10.4"W (LE).

and shallow-water intraclastic-bioclastic-peloidal facies on top (Fig. 4). New ammonite findings allowed the identification of the successive upper Bajocian biozones. Fossil sites BM-B and BM-C consists of the muddy deposits of the transgressive hemicycle of the sequence, within the *S. niortense* Zone, whereas BM-PI1 and BM-PI2 are also in muddy sediments but lateral to small patches, within the *G. garantiana* Zone. Muddy facies coeval with small patches were interpreted in Moscardón as deposited in the proximal deep ramp, at the upper part of the low-angle slope of the ramp, below or around storm wave base (Aurell and Bádenas 2015). Therefore, the palaeoenvironment of BM-PI1 and BM-PI2 corresponds to inter-patches sediments within this shallowest part of the deep ramp, at around 30–35 m in depth (Fig. 5). Concerning BM-B and BM-C, their location in muddy transgressive sediments indicates they formed in the deep ramp in either as inter-mound sediments or in areas without microbial-sponge mounds. Taxa in this site include ?*Pithonoton* sp., *Tanidromites ciceroides* Ferratges & Zamora sp. nov., and *T. monevaensis* Ferratges & Zamora sp. nov.

Lécera.—The outcrop located south of Lécera (coordinates: 41°09'33.6"N 0°44'10.4"W) in the Barranco de la Peñisquera, was described by Bulard (1972). Here only the upper part of the succession (upper Bajocian *G. garantiana* and *P. parkinsoni* ammonite zones) has been studied in detail due to few exposures available of the underlying lower Bajocian succession (Fig. 4). The upper Bajocian succession is formed mainly by deep ramp muddy facies (sponge-rich limestones, marly limestones, and marls) including 1 m-thick microbial-sponge patches at its uppermost part, reflecting a subtle shallowing tendency (from deep ramp to close to the slope). Fossil sites LE-1 to LE-3 correspond to this uppermost and shallowest part of the succession, i.e., in interpatch sediments, a palaeoenvironmental position belonging to the upper part of the low-angle ramp slope, similar to BM-PI1 and BM-PI2 of Moneva, i.e., 30–35 m in depth (Fig. 5). Crab species in this site include *Iberophthalmus leceraensis* Ferratges & Zamora gen. et sp. nov., *Tanidromites ciceroides* Ferratges & Zamora sp. nov., and *Tanidromites* cf. *raboeufi* Robin et al., 2015.

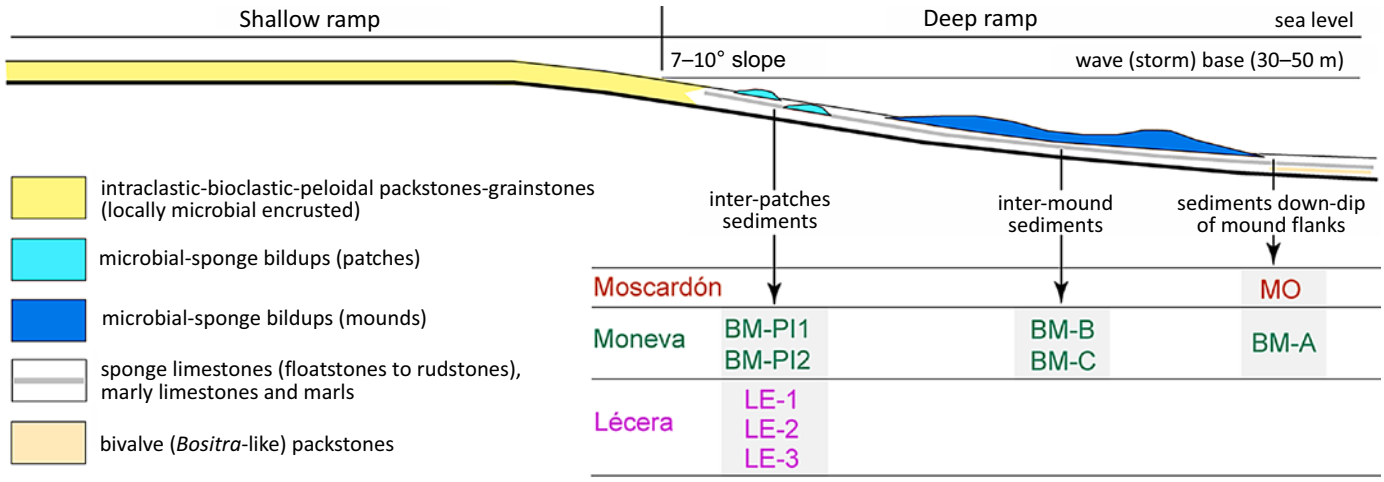

Fig. 5. Palaeoenvironmental reconstruction of the Bajocian facies in the Iberian Basin, within a distally-steepened carbonate ramp (modified from Bádenas and Aurell 2018: fig. 5b), indicating the location of the studied brachyuran fossil sites.

Systematic palaeontology

by Fernando Ari Ferratges and Samuel Zamora

Order Decapoda Latreille, 1802

Infraorder Brachyura Latreille, 1802

Section Dromiacea De Haan, 1833

Superfamily Homolodromioidea Alcock, 1900

Family Longodromitidae Schweitzer & Feldmann, 2009c

Genus *Iberophthalmus* Ferratges & Zamora gen. nov.

Zoobank LCID: urn:lsid:zoobank.org:act:07697263-E685-48AB-A3E3-2A6E1C3CA130.

Etymology: Combination of Iberia, in reference to the oldest known occurrence of brachyurans from the region, and the Greek *ophthalmos* (ὀφθαλμός), eye, referring to the deep orbital cavities.

Type species: *Iberophthalmus leceraensis* Ferratges & Zamora gen. et sp. nov., by monotypy; see below.

Diagnosis.—As for the monotypic type species.

Remarks.—Some Middle Jurassic genera, such as *Eodromites* Patrulius, 1959 (see examples in Starzyk 2015), *Laeviprosopon* (von Meyer, 1860), *Bajoprosopon* Van Bakel et al., 2021, and *Meroncarcinus* Van Bakel & Guinot, 2023, show superficial similarities to *Iberophthalmus* n. gen. However, they can be readily distinguished by differences in the shape and distribution of grooves and dorsal regions.

The genus showing the greatest overall morphological similarity to the new material is *Abyssophthalmus* Schweitzer & Feldmann, 2009c (included within the family Longodromitidae Schweitzer & Feldmann, 2009c). Both share a markedly convex carapace with relatively deep, well-ornamented orbits and well-defined dorsal regions. Nevertheless, *Iberophthalmus* Ferratges & Zamora gen. nov. differs from *Abyssophthalmus* in having a wider spacing between the cervical and branchiocardiac grooves, a general outline with a narrower posterior third, a narrow and depressed intestinal region, more concave and deeper dorsal grooves, and more distinctly defined dorsal regions (see Schweitzer and Feldmann 2009a).

Other Middle Jurassic genera assigned to the Longodromitidae, such as *Planoprosopon* Schweitzer et al., 2007, and *Coelopus* Étallon, 1861, as well as Upper Jurassic taxa such as *Pilidromia* Schweitzer et al., 2018, also share superficial similarities, including the general outline and the shape and distribution of the dorsal regions, as well as relatively deep orbits. However, all of these genera differ in possessing a more inflated and less convergent posterolateral margin than *Iberophthalmus* gen. nov., in addition to subtle differences in the distribution, shape, and size of the dorsal regions.

Based on this combination of characters, together with those shared with *Abyssophthalmus*, the family Longodromitidae is regarded as the most appropriate systematic placement for the new genus. This suite of characteristics is consistent with the diagnosis of the Longodromitidae as proposed by Schweitzer and Feldmann (2009c).

In addition, other genera included within Longodromitidae from younger strata show certain similarities to the new genus. *Antarctiprosopon* Schweitzer & Feldmann, 2011, from the Eocene of Antarctica, superficially resembles the new genus in overall outline and in the distribution of dorsal regions. However, the new genus clearly differs from *Antarctiprosopon* in the configuration of its grooves, its ornamentation, more strongly arched lateral margins, and a markedly more concave posterior margin.

Cuchiadromites Ossó et al., 2021, from the Aptian of Spain, shares some similarities in the anterior half of the carapace, including the shape and arrangement of grooves and dorsal regions, as well as a strongly developed urogastric region. Nevertheless, the new genus lacks a postcervical groove, and the branchial groove is more strongly marked and continuous with the cardiac region, unlike in *Cuchiadromites*.

Garrafosopon Ossó, Van Bakel, & Artal in Ossó et al., 2023, from the Aptian of Spain, also exhibits an elongated outline and a broadly similar distribution of dorsal regions.

However, it differs from the new genus in having much less defined dorsal grooves, a considerably larger outer orbital spine, and a more rectangular outline.

Rosadromites Schweitzer et al., 2016, also shows similarities to the new genus, including an elongated outline, comparable shape and distribution of dorsal regions, a swollen urogastric region, well-marked branchiocardiac grooves, and a triangular posterior margin of the cardiac region. It differs, however, in having less distinct dorsal grooves and ornamentation, well-defined hepatic regions, and a posterior margin that is wider than that of the new genus.

Longodromites Patrulius, 1959, shares similarities with the new genus in having an elongated, oval outline and generally well-defined regions. However, species assigned to *Longodromites* display a less defined mesogastric region, a more posteriorly positioned cardiac region located behind the branchial groove (rather than continuous with it as in the new genus), and a swelling on the outer side of the branchiocardiac groove.

These similarities with several genera within Longodromitidae further support its placement within the family.

Stratigraphic and geographic range.—As for the type and only species.

Iberophthalmus leceraensis Ferratges & Zamora sp. nov.

Zoobank LCID: urn:lsid:zoobank.org:act:7B9B1530-7BC4-463A-9AB5-D3A89C386AE4.

Etymology: In reference to the village of Lécera, Spain, where the fossil-bearing locality that yielded the material is located.

Holotype: MPZ 2025/303, an almost complete carapace of 6.2 mm width, and 8.9 mm length (with incomplete rostrum, see Fig. 6).

Type locality: Lécera (sites LE-1 and LE-2), Zaragoza province, Spain.

Type horizon: *Parkinsonia parkinsoni* Ammonite Zone, Upper Bajocian, Middle Jurassic.

Material.—Holotype (MPZ 2025/303), almost complete carapace corresponding to an external mould (MPZ 2025/304), a poorly preserved and decorticated specimen from the type locality and horizon.

Diagnosis.—Carapace longer than wide, moderately vaulted both transversely and longitudinally. Rostrum wide, long (incomplete), sulcate, with flared lateral margins and a markedly downturned tip; orbits deep, directed anterolaterally; outer orbital spine small, directed anterolaterally. Cervical and branchiocardiac grooves deep; postcervical groove composed of two distinct segments. Lateral margins approximately parallel, bearing small spines. Subhepatic region well developed. Dorsal carapace ornamentation granular.

Description.—Carapace longer than wide, CL/CW = 1.4, widest at the epibranchial region, approximately at the mid-length of the carapace; carapace domed both transversely and longitudinally; dorsal regions well defined by grooves and granular ornamentation. The rostrum is broad, with the basal width slightly less than half the maximum carapace width; axially grooved, inclined downward; lateral margins gently rounded but neither expanded nor channelled as in other species. Augenrests directed anterolaterally; the outer orbital spine is short, directed anterolaterally; fronto-orbital width is approximately 90% of the maximum carapace width. Lateral margins are convex, ornamented with small spines. Posterior margin is concave and bordered (see Fig. 6A_1 and B).

Epigastric regions slightly inflated, located at the base of the rostrum. Protogastric regions inflated, granular, with tubercles of varying sizes; hepatic regions nearly undifferentiated. Mesogastric region triangular posteriorly, with a long anterior process ending at the base of the rostrum. Metagastric region broader than the mesogastric, axially constricted, posteriorly bounded by the postcervical groove. Urogastric region developed only as a broad groove, depressed below the level of the metagastric region. Cardiac region is inflated, with an inverted subtriangular shape. Cervical groove is deep, slightly sinuous; postcervical groove nearly continuous across the central part of the carapace; branchiocardiac groove

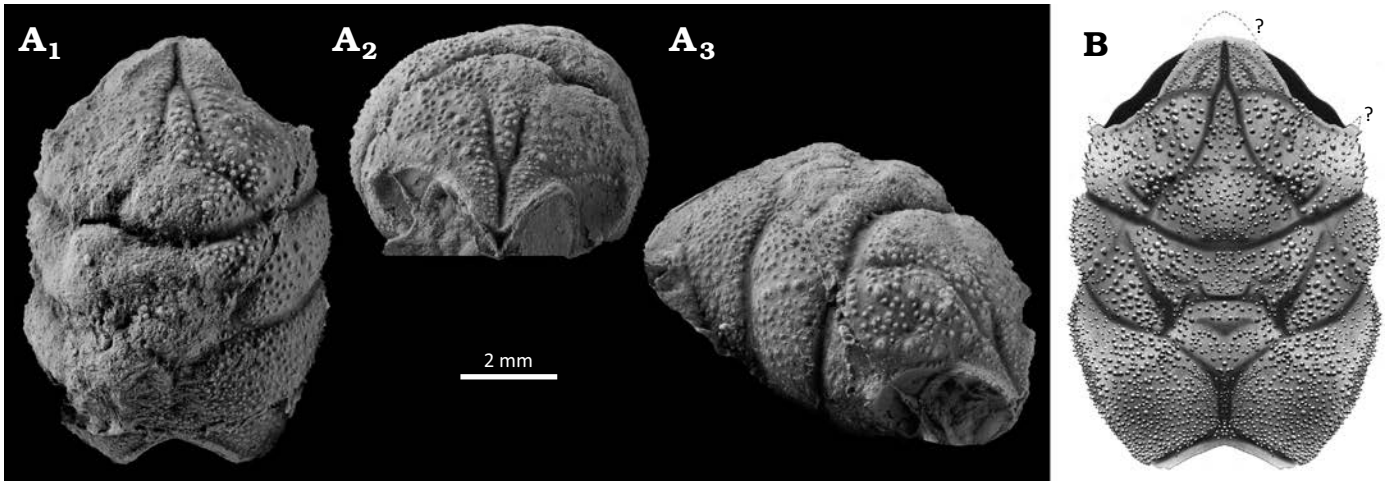

Fig. 6. Homolodromioidean crab *Iberophthalmus leceraensis* Ferratges & Zamora gen. et sp. nov. from the upper Bajocian of Lécera, Spain. **A**. MPZ 2025/303 (holotype) latex cast of the specimen (whitened with ammonium chloride) in dorsal (A_1), frontal (A_2), and oblique lateral (A_3) views. **B**. Idealised reconstruction.

oblique, extending toward the cardiac region. Epibranchial region broad, with an oval swelling near the cardiac region. Remaining branchial regions undifferentiated, densely granular overall, with smaller granules in the posterior third. Branchiocardiac and postcervical grooves extend laterally.

Remarks.—The new species is similar to *Abyssophthalmus bellaii* (Crônier & Boursicot, 2009) in the shape and arrangement of the dorsal regions, the orbito-frontal margin, and the strongly concave posterior margin. However, the new species has a much broader mesogastric and epibranchial region, and a significantly narrower posterior margin. Material assigned to *A. hebes* by von Meyer (1840), although highly fragmentary, also shows similarities in the shape and distribution of the dorsal regions, but can be distinguished from the new species by its more pronounced postcervical groove and mesogastric lobes, which are much more developed than in *Iberophthalmus leceraensis* Ferratges & Zamora gen. et sp. nov. *Abyssophthalmus mainense* (Crônier & Boursicot, 2009) can be clearly differentiated from the new species by its more rectangular outline and less defined dorsal regions.

Stratigraphic and geographic range.—Upper Bajocian, *P. parkinsoni* Ammonite Zone (Fig. 4), sites LE-1 and LE-2 of Lécera, Spain.

Family Tanidromitidae Schweitzer & Feldmann, 2008

Genus *Tanidromites* Schweitzer & Feldmann, 2008

Type species: *Prosopon insigne* von Meyer, 1860, by original designation, from Fürsitz (near Aalen-Wasseralfingen, Germany), Middle Oxfordian to latest Kimmeridgian.

Species included: *Tanidromites aequilatus* (von Meyer, 1857), [as *Prosopon*]; *Tanidromites alexandrae* Starzyk, 2015; *Tanidromites ciceroides* Ferratges & Zamora sp. nov. (herein); *Tanidromites etalloni* (Collins in Collins & Wierzbowski, 1985) [as *Coelopus*]; *Tanidromites hyznyi* (Starzyk, 2015) [as *Eodromites*]; *Tanidromites insignis* (von Meyer, 1860) [as *Prosopon*]; *Tanidromites lithuanicus* Schweigert & Koppka, 2011; *Tanidromites longinosa* Starzyk, 2016; *Tanidromites maerteni* Fraaije et al., 2013; *Tanidromites monevaensis* Ferratges & Zamora sp. nov. (herein); *Tanidromites montreuilense* Crônier & Boursicot, 2009; *Tanidromites muelleri* Krobicki & Zatoń, 2016; *Tanidromites nightwishorum* Klompmaker et al., 2020; *Tanidromites pustulosa* (von Meyer, 1860) [as *Pithonoton*]; *Tanidromites raboeufi* Robin et al., 2015; *Tanidromites richardsoni* (Woodward, 1907) [as *Prosopon*]; *Tanidromites rotundus* (Starzyk, 2015) [as *Eodromites*]; *Tanidromites scheffnerae* Schweigert & Koppka, 2011 (= *Tanidromites wysokaensis* Starzyk, 2016); *Tanidromites schweitzerae* Starzyk, 2016; *Tanidromites sculpta* (Quenstedt, 1857) [as *Prosopon*] (= *Prosopon elongatum* von Meyer, 1857); *Tanidromites starzykae* Schweitzer et al., 2018; *Tanidromites weinschenki* Klompmaker et al., 2020.

Diagnosis.— For emended diagnosis see Starzyk (2016: 4).

Remarks.—The genus *Tanidromites*, is one of the most diverse during the Middle Jurassic (with six known species), and especially in the Late Jurassic, being particularly associated with environments containing sponge-microbial bioherms in the epicontinental seas of Europe (e.g., von Meyer 1860; Collins and Wierzbowski 1985; Wehner 1988; Müller et al. 2000; Garassino and Krobicki 2002; Schweitzer and Feldmann 2008; Hyžný et al. 2011; Starzyk 2013).

Several of the examined specimens from the three Middle Jurassic studied localities (Lécera, Moneva, and Moscardón) can be assigned to at least four different species of *Tanidromites* based on the characteristic features noted by different authors (Schweitzer and Feldmann 2008, 2009b; Starzyk 2013). In addition, in the last years, several authors (Robin et al. 2015; Krobicki and Zatoń 2016; Klompmaker et al. 2020) have discussed in detail the morphological differences among most known species of tanidromitids. The key features of this genus are: (i) carapace longer than wide; (ii) outline with parallel/subparallel margins; (iii) triangular-shaped front, with a long, strongly developed rostrum curving downward; (iv) groove pattern with well-defined hepatic, cervical, and postcervical lines; (v) clearly visible hepatic, mesogastric, and cardiac regions; (vi) shape and outline of the augenrest; (vii) posterior margin with a rounded rim, concave at the centre (see Starzyk 2016).

Stratigraphic and geographic range.—Lower upper Bajocian–Tithonian (Berriasian?) of Europe.

Tanidromites ciceroides Ferratges & Zamora sp. nov.

Figs. 7A, 8.

Zoobank LCID: urn:lsid:zoobank.org:act:7E275B4D-A60B-44F2-8098-DA8ECCFB1A51.

Etymology: From the Latin *cicer*, chickpea, and the suffix *-oides*, resembling; referring to the overall shape of the carapace, reminiscent of a chickpea.

Type material: The holotype: MPZ 2025/314, a complete carapace of 2.6 mm width, and 4.3 mm length (with rostrum). Paratypes: MPZ 2025/315–320 from the type locality and horizon.

Type locality: Moneva and Lécera site LE-1, Zaragoza province, Spain.

Type horizon: *Stephanoceras humphriesianum* to *Parkinsonia parkinsoni* ammonite zones, lower to upper Bajocian, Middle Jurassic.

Material.—Total of 16 specimens: 9 from Moneva (MPZ 2025/305–313) and 7 from Lécera (MPZ 2025/314–320), Spain; lower to upper Bajocian, *S. humphriesianum* to *P. parkinsoni* ammonite zones.

Diagnosis.—Small carapace, slightly oval, longer than wide, CL/CW = 1.5, vaulted both transversely and longitudinally; rostrum and augenrest margin armed with small spines; outer-orbital spine compound; lateral margins convex, lacking large lateral spines. Postcervical grooves shallow; dorsal surface densely ornamented with conical granulations; posterior half covered with paired granules.

Description.—Carapace suboval in outline, CL/CW = 1.5, maximum length in the fronto-orbital margin. Broad, rounded rostrum, armed with small spines, curved downward, with an axial sulcus. Augenrest broad, shallow, with small spines on the upper margin and a small compound outer-orbital spine. Outer margin of the hepatic region serrated, slightly swollen. Hepatic/mesogastric grooves well visible, extending posteriorly to the mesogastric region. Hepatic region sub-oval. Cervical groove deep and sinuous. Epibranchial region as wide as half of the branchial region, with anteriorly concave postcervical grooves, more visible

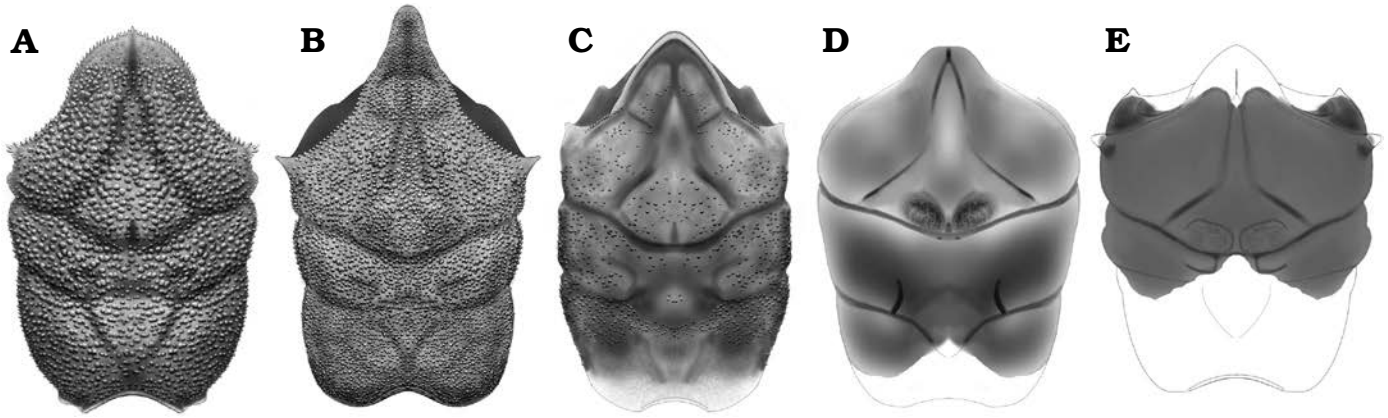

Fig. 7. Idealised reconstruction and comparison of the five species included in the homolodromioidean *Tanidromites* Schweitzer & Feldmann, 2008, from the three studied sites in Spain. **A**. *Tanidromites ciceroides* Ferratges & Zamora sp. nov. from the lower to upper Bajocian of Lécera. **B**. *Tanidromites monevaensis* Ferratges & Zamora sp. nov. from from the upper Bajocian of Moneva. **C**. *Tanidromites* cf. *monevaensis* Ferratges & Zamora sp. nov. from from the lower Bajocian of Moscardón. **D**. *Tanidromites* cf. *raboeufi* Robin et al., 2015, from the upper Bajocian of Lécera. **E**. *Tanidromites* sp. from the upper Bajocian of Moneva. Not to scale.

in the internal mould. Cardiac region triangular, not well defined. Branchiocardiac grooves shallow, more visible in the internal mould. Branchial region rhomboidal in outline. Posterior margin concave, with a small, rounded rim. Dorsal surface ornamented with thick conical granules, arranged in pairs in the central part from the posterior half onward. Internal mould granulated.

Remarks.—The new species is similar to *Tanidromites richardsoni* (Woodward, 1907), showing significant similarities in the carapace outline, ornamentation composed of granules, and overall appearance. However, it differs in the size of the epibranchial region, which is narrower and less rectangular in the new species; the branchial groove is more oblique than in the new species, with the arching over the cardiac region less abrupt in *T. richardsoni*; the mesogastric groove in the new species is deeper; the postcervical groove is less marked in the new species and lacks the two tubercles in the cardiac region that *T. richardsoni* possesses. The posterior third is narrower in the new species. Additionally, the granulation of *T. ciceroides* Ferratges & Zamora sp. nov. is notably thicker (although this could be an ontogenetic trait; when comparing the large specimen from Lécera with *T. richardsoni*, we observe that the grooves are much less marked, and the orientation of the grooves does not match, see below).

Tanidromites muelleri Krobicki & Zatoń, 2016, also shows similarities with the new species in its general morphology. However, *T. muelleri* has a much more rectangular and compact outline, with a much narrower and more pointed rostrum compared to *T. ciceroides* Ferratges & Zamora sp. nov., and the branchial region is wider than in the new species; the epibranchial region of *T. muelleri* is wider, with the postcervical groove more marked than in the new species, and it also carries a spine on the lateral margin, which the new species lacks. Finally, *T. ciceroides* Ferratges & Zamora sp. nov. does not present significant dorsal knobs, unlike *T. muelleri*.

The other *Tanidromites* species from the Middle Jurassic (*Tanidromites maerteni* Fraaije et al., 2013; *Tanidromites montreuilense* Crônier & Boursicot, 2009; *Tanidromites lithuanicus* Schweigert & Koppka, 2011; and *Tanidromites raboeufi* Robin et al., 2015; and the new species *Tanidromites monevaensis* Ferratges & Zamora sp. nov. and *Tanidromites* cf. *monevaensis* Ferratges & Zamora sp. nov., as well as those from the Late Jurassic age, are excluded from the comparison due to being clearly distinct in outline, ornamentation, and general parameters (like length and width of the dorsal regions and inclination of the dorsal grooves).

Some specimens of the new species have been identified, presumably representing different ontogenetic stages (Fig. 8E–G). These specimens display a very similar overall morphology, maintaining consistent proportions of the carapace outline, grooves, and dorsal regions. However, a gradual reduction in the size of the ornamentation and in the depth of the dorsal grooves is observed in largest specimens. On this basis, all specimens are here interpreted as representing different ontogenetic stages of the same species.

Stratigraphic and geographic range.—Lower to upper Bajocian, *S. humphriesianum* to *P. parkinsoni* ammonite zones, sites BM-A, BM-B, BM-C and BM-PI1 and BM-PI2 of Moneva and sites LE-2 and LE-3 of Lécera, Spain (Fig. 4).

Tanidromites monevaensis Ferratges & Zamora sp. nov.

Figs. 7B, 9.

Zoobank LCID: urn:lsid:zoobank.org:act:F4AF4571-0D5A-4ACA-9DC6-691FF11E1EFA.

Etymology: In reference to the locality where the specimens were found.

Type material: The holotype: MPZ 2025/321, a complete carapace of 3.6 mm width, and 5.5 mm length (with rostrum). Paratypes: MPZ 2025/322–324 from the type locality and horizon.

Type locality: Moneva, Zaragoza province, Spain.

Type horizon: *Strenoceras niortense–Garantiana garantiana* ammonite zones, Upper Bajocian, Middle Jurassic.

Material.—Total of 46 specimens (MPZ 2025/321–366) from the type locality and horizon.

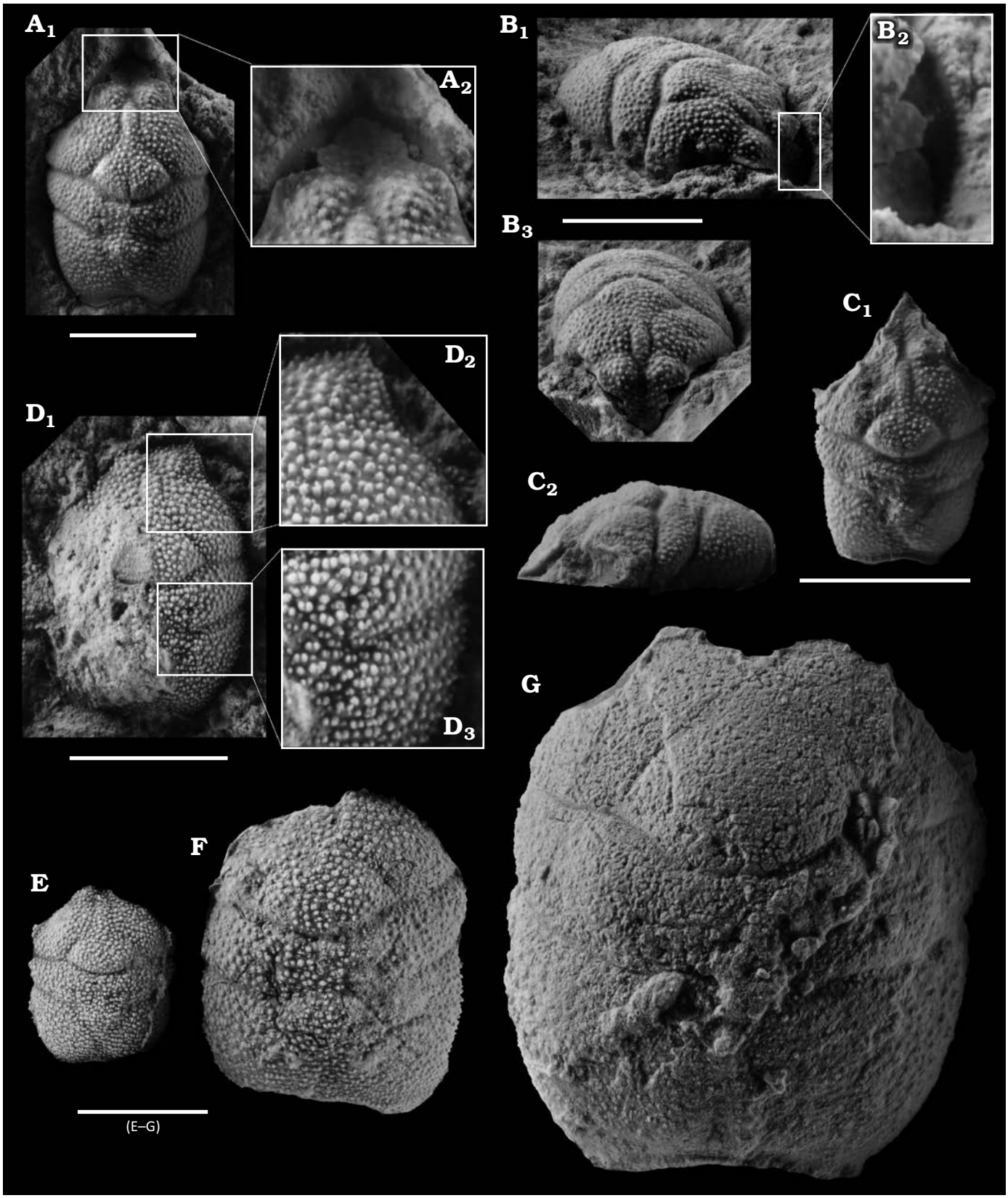

Fig. 8. Homolodromioidean crab *Tanidromites ciceroides* Ferratges & Zamora sp. nov. from the lower to upper Bajocian of Lécera, Spain. **A**. Holotype MPZ 2025/314 in dorsal view (A_1), detail of the rostrum (A_2), note the spines on the margin. **B**. Paratype MPZ 2025/315 in oblique lateral (B_1) and oblique frontal (B_2), detail of the rostrum (B_3). **C**. Paratype MPZ 2025/316 in dorsal (C_1) and left lateral view (C_2). **D**. Latex cast of MPZ 2025/317 in dorsal view (D_1) with details of dorsal ornamentation (D_2, D_3). **E**–**G**. MPZ 2025/318–320, respectively, specimens at different ontogenetic stages (E, F latex casts). All specimens have been whitened with ammonium chloride sublimated for photography. Scale bars 2 mm.

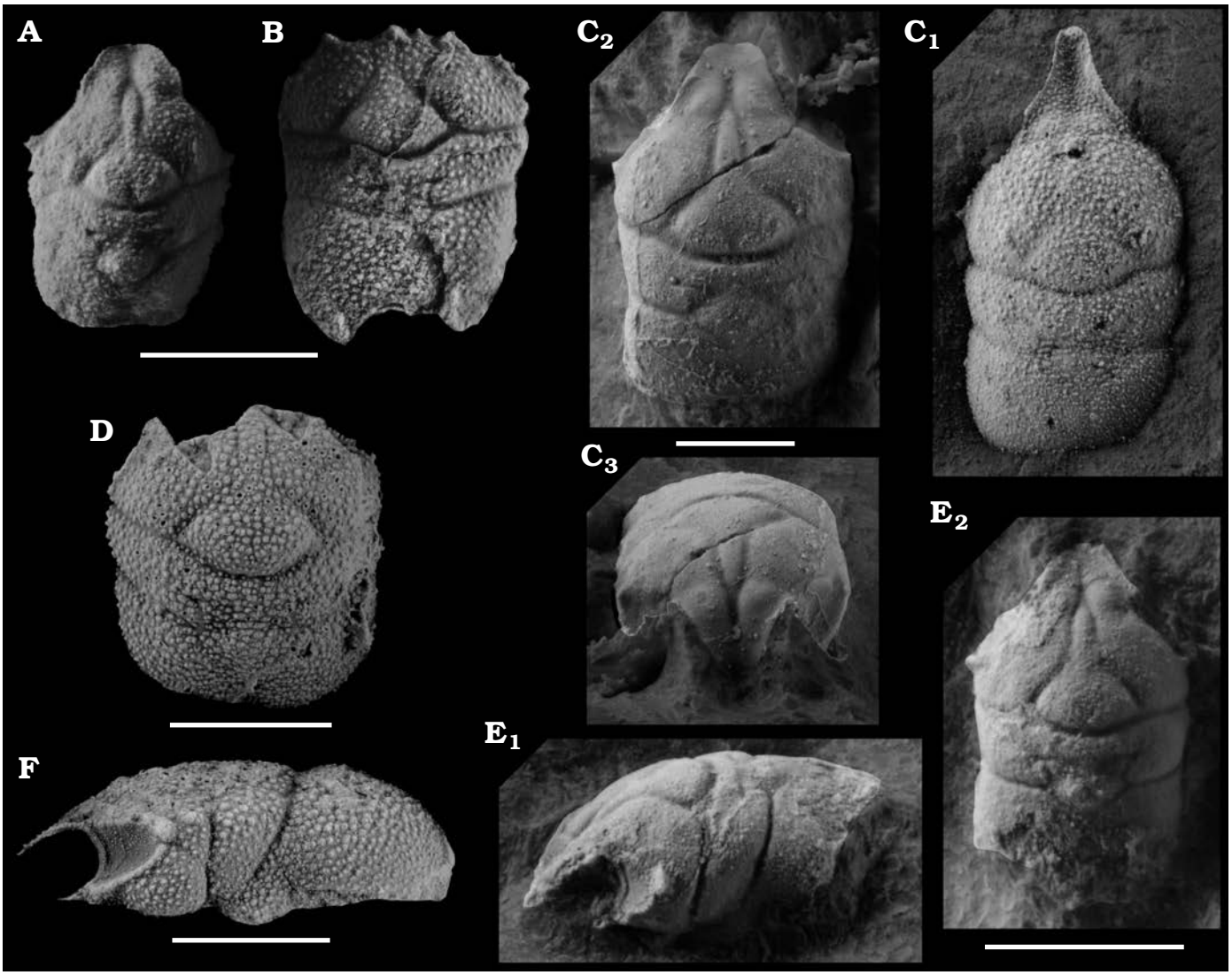

Fig. 9. Homolodromioidean crab *Tanidromites monevaensis* Ferratges & Zamora sp. nov. from the upper Bajocian of Moneva, Spain. A, B. Two specimens in the same matrix (MPZ 2025/325, 326). C. Holotype MPZ 2025/321 in dorsal view: external mould latex cast (C_1), internal mould (C_2), frontal view of the internal mould (C_1). **D**. MPZ 2025/322 latex cast in dorsal view. **E**. MPZ 2025/323 in left lateral (E_1) and dorsal (E_2) views. F. MPZ 2025/324 latex cast in left lateral view. All specimens have been whitened with ammonium chloride sublimated for photography. Scale bars 2 mm.

Diagnosis.—Subrectangular shape, with very distinct, long rostrum, greater width in the anterior part; CL/CW = 1.49 in the internal mould and 1.57 in the external mould; distinctive grooves, granulation of whole carapace surface (not in the internal mould); Dorsal regions without knobs.

Description.—Carapace subrectangular in outline, CL/CW = 1.49 in the internal mould and 1.57 in the external mould; maximum length in the fronto-orbital margin. Long, broad, downturned triangular rostrum, with axial sulcus, shorter in the inner mould. Augenrest developed, weakly defined, very shallow with small outer orbital spine. Outer margin of hepatic region short, slightly convex. Hepatic grooves well visible, continued posteriorly to mesogastric region. Hepatic region sub-oval. Cervical groove relatively deep, sinuous. Epibranchial region narrow with anteriorly-concave postcervical grooves, more visible in the internal mould. Cardiac region triangular, not well defined. Branchiocardiac grooves shallow, more visible in the internal mould. Branchial region rhomboidal in outline, narrower posteriorly. Posterior margin concave, with small, rounded rim. Dorsal ornamentation consisting of granules covering the entire surface, simple and rounded in the anterior third, and arranged in pairs in the central area, from the cervical groove to the posterior margin. The internal mould is smooth, without clear evidence of the granulation (Fig. 9C).

Remarks.—The new species bears a superficial resemblance to *Tanidromites muelleri* Krobicki & Zatoń, 2016, from the uppermost Bajocian of Kawodrza Górna, Polish Jura. However, the new species differs from *T. muelleri* by its smaller extra-orbital spine, more elongated rostrum, narrower posterior margin, and the absence of well-developed knobs as seen in *T. muelleri*. Additionally, the new species has a narrower and slenderer outline than *T. muelleri*, with a small granulated epibranchial margin, lacking spines.

The studied material shows similarities with the material figured by Schweitzer and Feldmann (2008) and assigned to *T. lingulata* (von Meyer, 1857) (now *T. sculpta* after Klompmaker et al., 2020). However, the new material presents differences in the mesogastric region, which is more oval, the upper margin of the augenrest and the continuous rostrum, a broader protogastric-hepatic region, and a less perpendicular cervical groove compared to *T. sculpta*.

Tanidromites richardsoni (Woodward, 1907) differs from *T. monevaensis* Ferratges & Zamora sp. nov. in having finer ornamentation on internal mould and a more defined postcervical groove in *T. richardsoni*, as well as a more distinct cardiac region compared to *T. monevaensis* Ferratges & Zamora sp. nov.

The species *T. ciceroides* Ferratges & Zamora sp. nov. (described above), differs from *T. monevaensis* Ferratges & Zamora sp. nov. in having a narrower epibranchial coarser dorsal ornamentation and a less marked postcervical groove. The rostrum of *T. monevaensis* Ferratges & Zamora sp. nov. is narrower than that of *T. ciceroides* Ferratges & Zamora sp. nov. Additionally, the internal mould of both species can be distinguished by the presence of granulation in *T. ciceroides* Ferratges & Zamora sp. nov. and its absence in *T. monevaensis* Ferratges & Zamora sp. nov.

Tanidromites alexandrae Starzyk, 2015, from the Oxfordian of Poland, presents an internal mould very similar to the new species. However, unlike the latter, the Polish species has a much less defined mesogastric region, a shorter rostrum, and more sinuous orbits.

As in the previous case, the other *Tanidromites* species from the Middle Jurassic (as well as those from the Late Jurassic) are clearly distinct, as they are morphologically very different.

Stratigraphic and geographic range.—Upper Bajocian, *S. niortense–G. garantiana* ammonite zones, sites BM-C, BM-PI1, and BM-PI2 of Moneva, Spain (Fig. 4).

Tanidromites cf. *monevaensis* Ferratges & Zamora sp. nov.

Figs. 7C, 10.

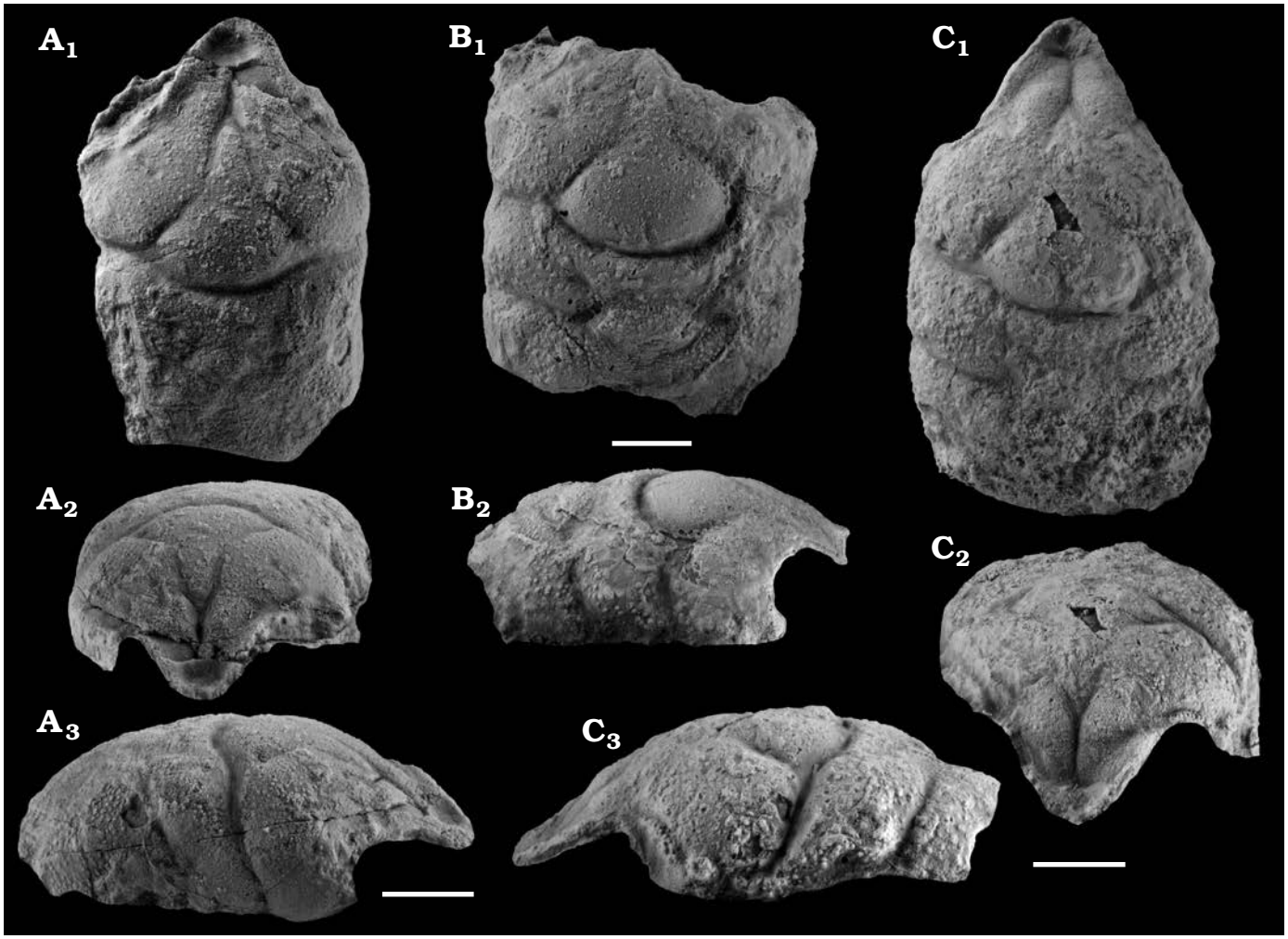

Fig. 10. Homolodromioidean crab *Tanidromites* cf. *monevaensis* Ferratges & Zamora sp. nov. from the lower Bajocian of Moscardón, Spain. **A**. MPZ 2025/367 in dorsal (A_1), frontal (A_2), and right lateral (A_3) views. B. MPZ 2025/368 in dorsal (B_1) and right lateral (B_2) views. **C**. MPZ 2025/369 in dorsal (C_1), oblique frontal (C_2), and left lateral (C_3)views. All specimens have been whitened with ammonium chloride sublimated for photography. Scale bars 2 mm.

Material.—Three specimens with cuticle (MPZ 2025/367–369): MPZ 2025/367, approx. 8.0 mm length (with rostrum), 6.1 mm width; MPZ 2025/368, approx., 8.1 mm width; MPZ 2025/369, approx. 11.0 mm length (with rostrum), 7.0 mm width from Moscardón, Spain; Lower Bajocian.

Description.—Carapace longitudinally and transversely convex, longer than wide, with subparallel lateral margins, slightly rounded and converging posteriorly (Fig. 10), without an external orbital spine. Rostrum elongated, spatulate subtriangular, with a raised edge, centrally sulcate, but the sulcus does not reach the tip (Fig. $10A_1$). The orbitofrontal margin is continuous, weakly concave, with a fairly pronounced angle; augenrest dorsally bordered with a row of small, aligned granules (Fig. 7C, $10C_2$, C_3). Mesogastric region well defined, oval, with a central groove at the posterior part; hepatic regions are undefined. No hepatic pits or tubercles are observed. The cardiac region is weakly vaulted, subpentagonal. Cervical groove is sinuous, with a wide arc in the centre. The branchiocardiac groove is clearly defined only in the outer third, subparallel to the cervical groove, shallow, as a weakly curved line; postcervical groove present. The cuticle is preserved, ornamented with small well-separated granules.

Remarks.—The three specimens of *Tanidromites* cf. *monevaensis* Ferratges & Zamora sp. nov. show significant morphological similarities with *T. monevaensis* Ferratges & Zamora sp. nov. described herein, particularly in carapace outline and in the shape and distribution of the dorsal regions. Nevertheless, *T.* cf. *monevaensis* Ferratges & Zamora sp. nov. exhibits some differences, including slightly convex lateral margins resulting in a less rectangular outline; an apparently shorter, more robust and rounded rostrum; dorsal regions more clearly defined by deeper grooves; and an apparently less granulated dorsal surface. For these reasons, the specimens from Moscardón are tentatively and with reservations assigned to the species described from equivalent stratigraphic levels at Moneva, pending the discovery of additional, better-preserved material.

Tanidromites cf. *raboeufi* Robin et al., 2015

Figs. 7D, 11.

Material.—One specimen without cuticle, MPZ 2025/370, approx. 7.0 mm length (with rostrum), 5.4 mm width, from Lécera (site LE-2), Spain, Upper Bajocian, *P. parkinsoni* Ammonite Zone.

Diagnosis.—See Robin et al. (2015: 181).

Description.—Carapace longer than wide, longitudinally and transversely convex, with subparallel margins that converge slightly posteriorly (Fig. 11). Margins gently rounded. Rostrum long, sulcate, subtriangular, with a blunt tip. Orbitofrontal margin continuous, slightly concave, not interrupted by the rostro-frontal groove, with a pronounced angle, without an apparent rim. Orbits poorly preserved, lacking an outer orbital spine. Epigastric regions obsolete; mesogastric region weakly defined, except anteriorly at the mesogastric process, with a broad, triangular base; hepatic regions undefined. Cervical pits subcircular; no hepatic pits or tubercles. Cardiac region weakly vaulted, subpentagonal, with two low nodules aligned horizontally. Cervical groove entire, sinuous, broadly arched medially. Branchiocardiac groove clearly defined only in the outer third, subparallel to the cervical groove, shallow.

Fig. 11. Homolodromioidean crab *Tanidromites* cf. *raboeufi* Robin et al., 2015 (MPZ 2025/370) from the upper Bajocian of Lécera, Spain. Specimen has been whitened with ammonium chloride sublimated for photography.

Remarks.—MPZ 2025/370 shows obvious differences compared to other *Tanidromites* species found in Moneva and Lécera, especially in the size and shape of the epibranchial region (much wider), straighter lateral margins, a wider and shorter mesogastric region, and less oval in shape. Unfortunately, since it is only an incomplete internal mould, a detailed comparison with other taxa cannot be made. However, the preserved overall morphology and preserved muscle scars (see Klompmaker et al. 2019 for details) shows important similarities with *Tanidromites raboeufi* Robin et al., 2015. The only noticeable difference between the specimen from the upper Bathonian of France (Robin et al. 2015: fig. 2) and the specimen from upper Bajocian of Lécera (Figs. 7, 11) is that the French species seems to have a slightly longer and narrower rostrum, and the anterior margin is somewhat more

inclined than in the Spanish material. Therefore, it is tentatively assigned to the same species.

?*Tanidromites* sp.

Figs. 7E, 12.

Material.—One partial specimen, MPZ 2025/302, preserved part of the carapace: 3.5 mm length (estimated 5 mm), 3.9 mm width (estimated 4.5 mm) from Moneva (site BM-C), Spain from *S. niortense* Zone of upper Bajocian.

Description.—Maximum length in the fronto-orbital margin. Rostrum not preserved. Augenrest broad, shallow, with small ridge on the upper margin. Lateral margin of the hepatic region smooth, slightly swollen, with a strong outer-orbital spine. Hepatic/mesogastric grooves well visible. Hepatic and protogastric regions undifferentiated. Cervical groove deep and sinuous. Epibranchial region relatively narrow, with anteriorly concave postcervical grooves. Cuticle partially preserved. Branchiocardiac groove deep, almost perpendicular to the axis. Dorsal surface smooth.

Remarks.—The specimen is too fragmentary to allow a detailed comparison. However, the preserved fragment has the cervical, postcervical, and branchiocardiac grooves, delimiting the relatively narrow epibranchial region with an almost straight posterior margin; a broad protogastric region; dorsal surface without granulations; a wide augenrest reaching the lateral margin, bordered by a small ridge; a well-developed (though broken) outer orbital spine; lateral margins without lateral spines, posteriorly convergent, wider in the frontal part (Fig. 12). The specimen is similar to species of *Tanidromites*, especially *T. aequilatum* (von Meyer, 1860), but the hepatic groove is more pronounced in the new material, the cervical groove is more rounded in its axial part, and the lateral margin is more posteriorly convergent in specimen. Only some of the characteristics mentioned by Feldmann et al. (2006) and Schweitzer and Feldmann (2008) are present in the new material, but the characteristic shape, dimensions, groove pattern, and combination of other diagnostic features suggest its inclusion with doubts in *Tanidromites*.

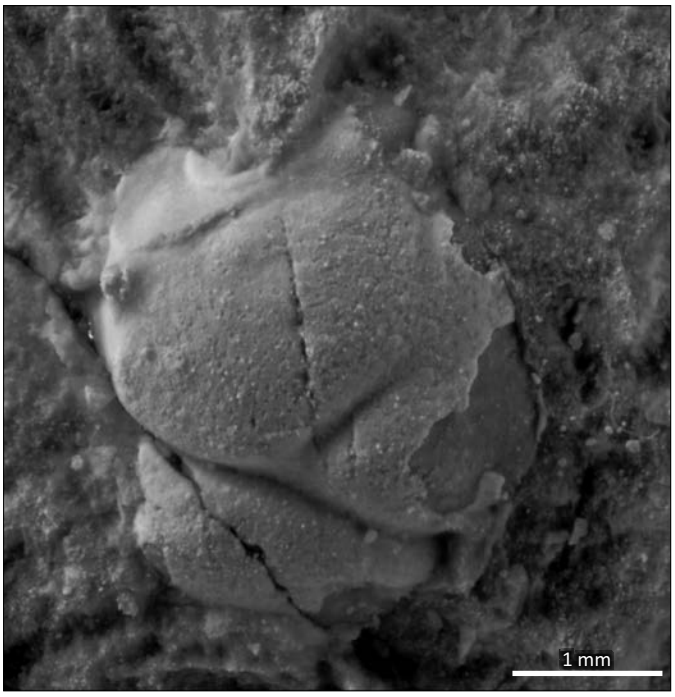

Fig. 12. Homolodromioidean crab *Tanidromites* sp. (MPZ 2025/302) from the upper Bajocian of Moneva, Spain. Specimen is whitened with ammonium chloride sublimated for photography.

Indeterminate isolated chelipeds

The taxonomic assignment of isolated chelipeds is challenging, because chelae are highly susceptible to convergent morphologies and therefore provide only a limited set of diagnostic features for precise identification (Collins 1999; Hyžný et al. 2015). Even so, isolated chelae are relatively common at Jurassic sites where dorsal carapaces of early brachyurans are also found (Hyžný et al. 2011, 2015). Despite this, such material has generally received little attention when occurring in loose association with Jurassic brachyurans (von Meyer 1860; Feldmann et al. 2006; Crônier and Boursicot 2009; Hyžný et al. 2011, 2015).

In addition to the diversity of carapaces of brachyuran crabs found in the studied outcrops, some isolated chelae have been collected, but these remains cannot be included in any known species. However, some remains show important similarities with materials reported by other authors. Two left propodi, lacking the dactyli (MPZ 2025/378, 379, Fig. 13H, I) of 3 mm in width and 7.4 mm in length (Fig. 13H), and 2.3 mm in width and 5.5 mm in length (Fig. 13I) show great similarities with material reported by Crônier and Boursicot (2009) from the lower Callovian (Middle Jurassic) of France. These chelae display an elongated, subrectangular palm with gently convex dorsal and ventral surfaces, a smoothly rounded outer margin, and a slightly carinate inner margin bearing a longitudinal row of tubercles. The fixed finger is relatively short, extending to about one-third of the palm's length. The articulation between the dactylus and the propodus is slightly oblique, and the base of the fixed finger measures roughly half the greatest width of the propodus. The dorsal surface of the propodus is ornamented with several longitudinal rows of tubercles. These specimens might well have belonged to a homolodromioid species as proposed by Crônier and Boursicot (2009). Other specimens (MPZ 2025/371–373, Fig. 13A–C) are similar to the specimens illustrated by Crônier and Boursicot (2009) from the lower Callovian of France. MPZ 2025/371–373 also show similarities with *Orhomalus medericki* Crônier & Boursicot (2009: pl. 2: 23–26), but the new material is decorticated and does not allow detailed comparisons.

One specimen, lacking the dactylus (MPZ 2025/377, Fig. 13G), of 4 mm in length and 1.8 mm in width, shows some similarities to the material described by Withers (1932) and refigured and described by other authors (Förster 1979; Feldmann and Schweitzer 2010; Scholtz 2020) from the Lower Jurassic of the UK, assigned to the *Eocarcinus*.

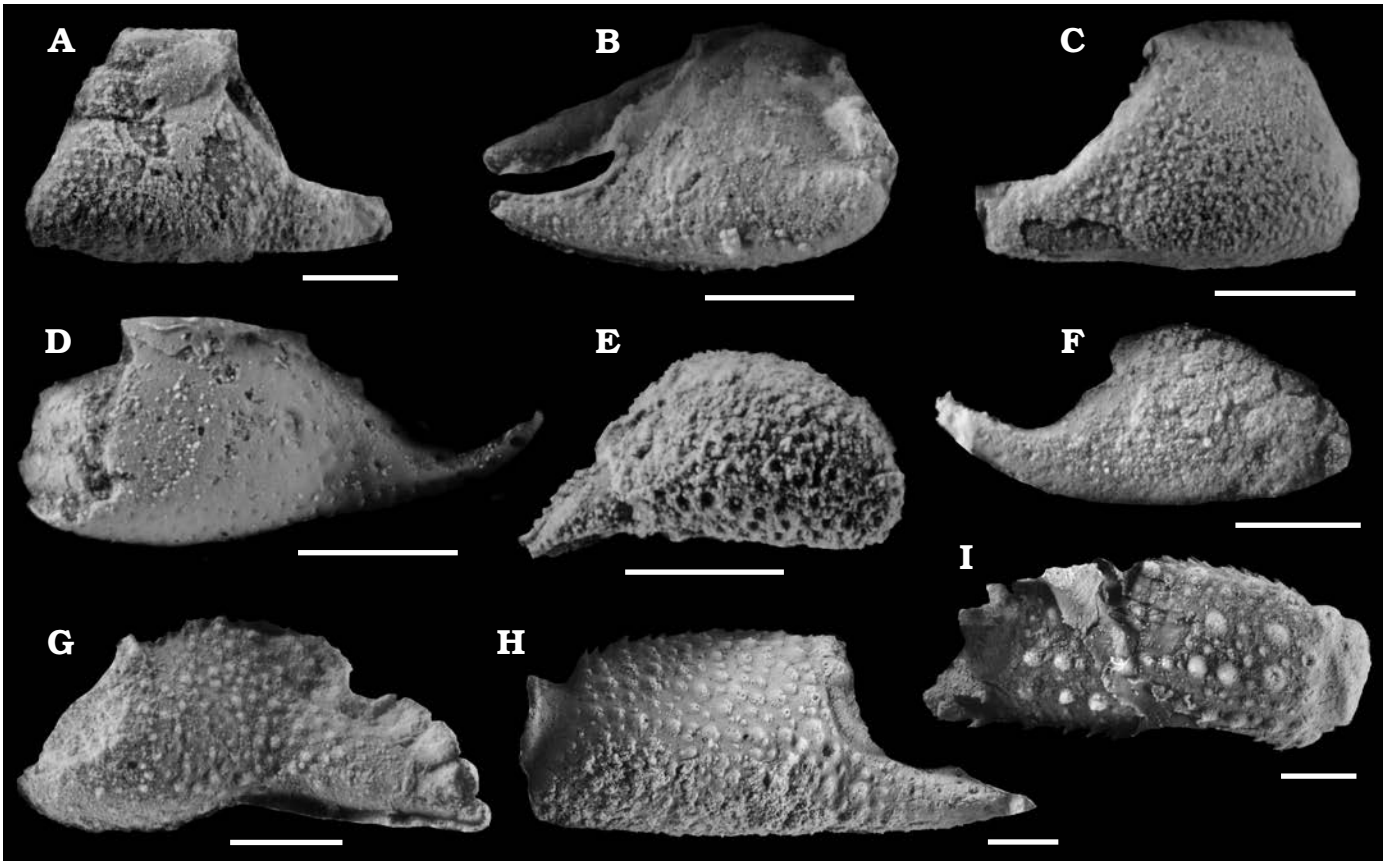

Fig. 13. Isolated propodi and chelae from the lower to upper Bajocian of Moneva (A–D) and Lécera (E–I), Spain. **A**. Left propodus MPZ 2025/371. **B**. Right chela MPZ 2025/372. **C**. Left propodus MPZ 2025/373. **D**–**F**. Isolated propodi MPZ 2025/374–376. **G**. Left propodus MPZ 2025/377. **H**, **I**. Right and left propodus (MPZ 2025/378 and MPZ 2025/379, respectively), similar to material illustrated by Crônier and Boursicot (2009), tentatively assigned to a homolodromioid species. Specimens D, H, I are latex casts. All specimens have been whitened with ammonium chloride sublimated for photography. Scale bars 1 mm.

Although the new material is much shorter, it shows some similar characteristics like: manus longer than high, surface with granules; fixed finger long and tall, lower margin is nearly straight, slightly downturned from manus, occlusal surface with prominent teeth, directed progressively more distally, terminating in distally directed tip. Other propodi (MPZ 2025/374–376, Fig. 13D–F) do not present distinctive elements and are not in a good state of preservation, so systematic comparisons cannot be made until more material is available for comparison.

Discussion

The distribution of brachyurans in the Middle Jurassic of the central Iberian Chain is not homogeneous (Table 3). They concentrate in muddy sediments lateral to microbial-sponge buildups of variable size in contrast to other Tethyan localities in which they have been reported associated to oolitic limestones and reef facies (facies 1 and 2 in Fig. 14). Only in the Late Jurassic brachyurans concentrate in sponge-coral buildups in other Tethyan areas (facies 3 in Fig. 14;

Table 3. Summary of the studied taxa from Spain, with stratigraphic and location information. N°, specimens

Taxa	Locality	Sequence	Site	Ammonite Zone	Age	N°
Iberophthalmus leceraensis Ferratges & Zamora gen. et sp. nov.	Lécera	Baj-2	LE-1 and LE-2	*Parkinsonia parkinsoni*	upper Bajocian	2
Tanidromites ciceroides Ferratges & Zamora sp. nov.	Moneva and Lécera	Baj-1–Baj-2	BM-A; BM-B; BM-C; BM-PI1 and BM-PI2; LE-2; LE-3	*Stephanoceras humphriesianum* to *Parkinsonia parkinsoni*	lower–upper Bajocian	16
Tanidromites monevaensis Ferratges & Zamora sp. nov.	Moneva	Baj-2	BM-C; BM-PI1; BM-PI2	*Strenoceras niortense* and *Garantiana garantiana*	lower–upper Bajocian	46
Tanidromites cf. *monevaensis* Ferratges & Zamora sp. nov.	Moscardón	Baj-1	MO	*Stephanoceras humphriesianum*	lower Bajocian	3
Tanidromites cf. *raboeufi* Robin et al., 2015	Lécera	Baj-2	LE-2	*Parkinsonia parkinsoni*	upper Bajocian	1
Tanidromites sp.	Moneva	Baj-2	BM-C	*Strenoceras niortense*	upper Bajocian	1

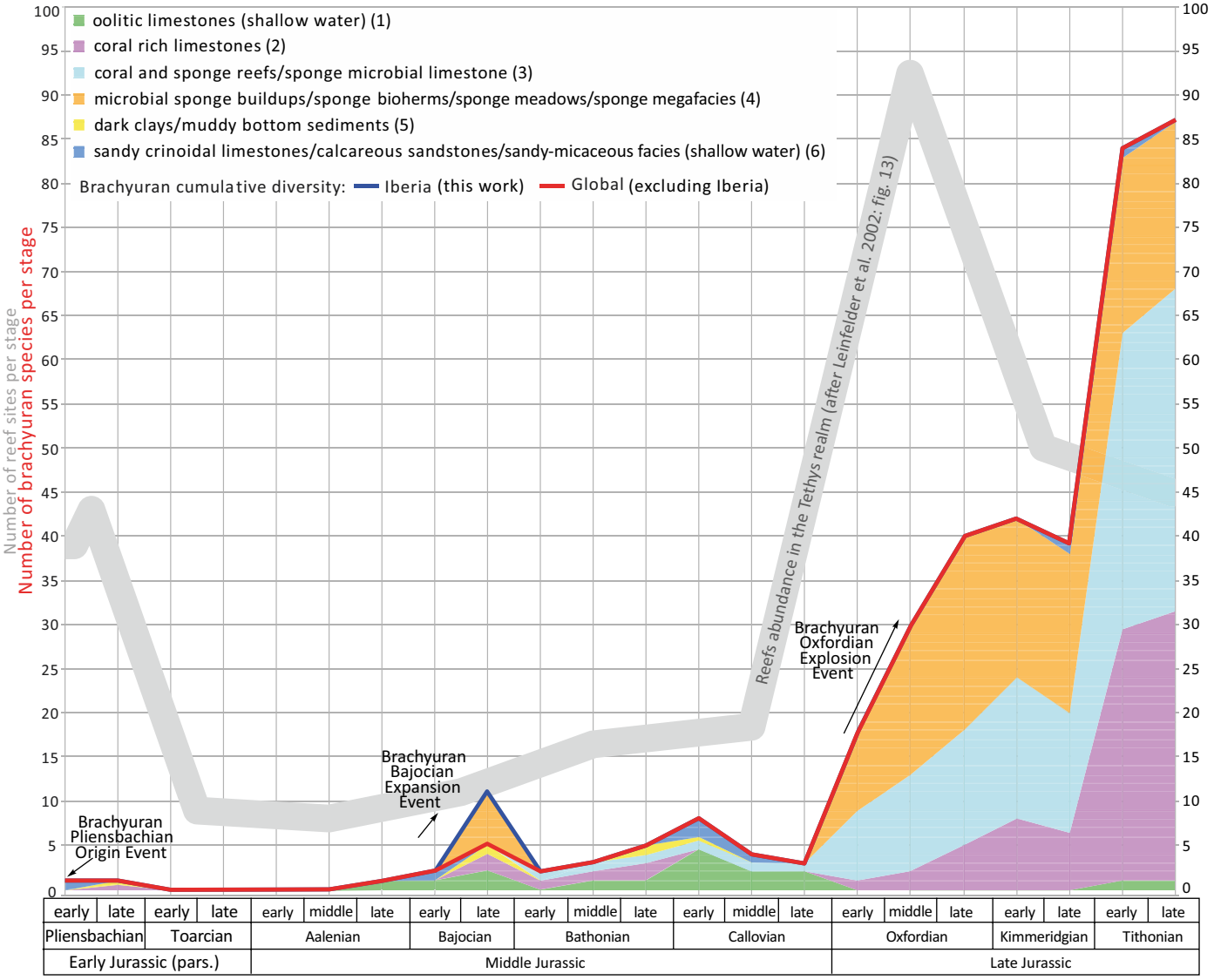

Fig. 14. Brachyuran's cumulative diversity and facies preference during the Jurassic compared to reefs abundance in the Tethys realm. Global curve (red) is mostly dominated by European records and does not include data from Iberia (blue). Reefs abundance in the Tethys curve has been constructed from data in Leinfelder et al. 2002: fig. 13. Time is not to scale.

i.e., Krobicki and Zatoń 2008, 2016). Number of specimens is also significantly larger compared to most of the reported localities and only Kawodrza Górna, central Poland (Krobicki and Zatoń 2016) shows a comparable number of specimens to the Iberian locality of Moneva. This suggests that sampling has been limited in those areas or alternatively taphonomy reduces the possibility to find complete brachyurans in such environments. But a true biological influence cannot be ruled out.

Specimens from Iberia, especially those from Moneva and Lécera, are generally complete but disarticulated, including not only carapaces but also chelipeds. Their occurrence within inter-patches and inter-mound sediments (see Fig. 15) suggests that the specimens lived and died close to the area in which they were finally buried, and can therefore be considered autochthonous or parautochthonous. Inter-patches and inter-mound sediments are areas that favoured preservation due to sediment accumulation after sedimentary events (i.e., storm events; Tomás et al. 2019; Aurell and Bádenas 2015). This suggests that individuals were living in the surrounding areas in large gregarious colonies, probably on the nooks and crannies of sponge buildups. These buildups of microbes and sponges of different shapes and sizes, may have provided suitable areas for feeding, settlement, and moulting.

The preservation of such material is variable depending on their palaeoenvironment. Brachyurans found in small microbial-sponge patches located in the upper part of the depositional slope (Fig. 5), concentrate around the patches and disappear laterally within only a few metres, suggesting minimal transport and supporting their autochthonous or parautochthonous nature. In contrast, material from mound-flank deposits (e.g., Moscardón) is comparatively rarer, more fragmentary, and largely limited to carapaces, sug-

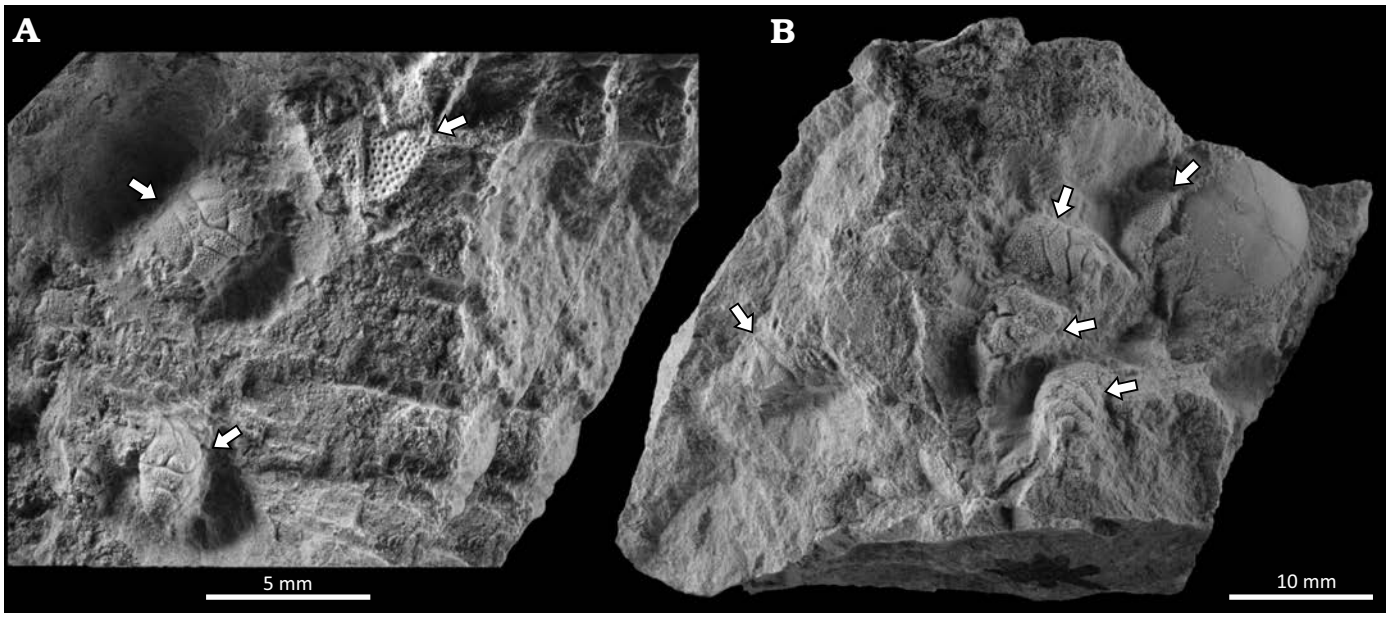

Fig. 15. Different matrices with decapod crustaceans from Bajocian of Moneva, Spain (BM PI1, Middle Jurassic) found in accumulations (**A**) or within sponges (**B**), along with buildups. White arrows indicate the different specimens preserved among the sponges.

gesting more transport (e.g., from the mound apex or around flanks where storm-induce down-dip density currents can potentially concentrate) or due to a longer exposure on the sea floor (e.g., due to lower sedimentation rates compared to the shallower sites at upper part of the depositional slope). This suggests that other Middle Jurassic decapods have not been evaluated much in the context of autochthony, since most published records consist of isolated and disarticulated elements (mainly carapaces).

Eocarcinus praecursor from the lower Pliensbachian of Gloucestershire (UK) is the oldest known brachyuran species, and its appearance is considered as the onset of the BPOE (Krobicki and Zatoń 2016). The next remarkable event in brachyuran history is the BBEE (Krobicki and Zatoń 2016; Van Bakel et al. 2021) when several new homolodromoids originated (Krobicki and Zatoń 2016). The Iberian new taxa described here almost double the previously known diversity of this group for the Bajocian, informing about when and how brachyurans diversified. Iberian brachyurans adapted to inhabit microbial-sponge buildups, a pioneering strategy for these crabs that only became more extensive in the peri-Tethyan basins during the Oxfordian onwards, with the expansion of the sponge-coralliferous environments (BOEE; sensu Krobicki and Zatoń 2016). As a consequence, this event also fuelled the expansion of "European" endemic taxa towards the reefal environments of Japan during the Late Jurassic (Krobicki and Zatoń 2016 and references therein).

There is also an apparent link between brachyurans diversity and coral reefs abundance (Fig. 14) showing a gradual increase from the Aalenian until the middle Callovian (if the BBEE is excluded), a drastic increase from the upper Callovian to the Oxfordian and a decrease in diversity in the Kimmeridgian coinciding with a rapid decline in reef abundance. However, it is noticeable the increase in diversity during the Tithonian when reef abundance seems to be declined according to the trend shown by Leinfelder et al. (2002). This might be explained due to the lack of precision in the dating of the Tithonian occurrences where almost all occurrences are imprecisely dated as Tithonian, so the records of this stage might be somehow duplicated since it is a cumulative diversity curve. But this circumstance needs to be further investigated.

Conclusions

Relatively diverse and in situ assemblages of brachyurans in the Middle Jurassic of Iberia are described based on relatively abundant material. Taphonomic evidence indicates that the studied Jurassic brachyurans are relatively autochthonous. Unlike most published material, which consists of disarticulated and isolated remains, these specimens occur lateral or within microbial-sponge buildups and disappear laterally, pointing to minimal transport and almost in situ preservation. Based on the sedimentological data, we interpret that crabs described here likely inhabited in the nooks and crannies of sponge buildups. This represents the earliest evidence of sponge buildups colonisation within brachyurans, since it has been only previously reported in the peri-Tethyan basins from the Oxfordian onwards, with development of the sponge-coralliferous environments.

A total of six taxa are described, four of them are new. With the Iberian brachyurans described here, we almost double previous diversity estimates of this group for the Bajocian, providing crucial information of when and how these crabs diversified during the Brachyuran Bajocian Expansion Event, likely by colonizing sponge buildups in the Western Tethys.

Acknowledgements

Isabel Pérez (Zaragoza, Spain) provided photographic assistance and Juan Carlos García Pimienta (Zaragoza, Spain) helped in the field work. We are also grateful to the reviewers Adiel Klompmaker (University of Alabama, Tuscaloosa, USA) and Günter Schweigert (Staatliches Museum für Naturkunde, Stuttgart, Germany) who greatly improved the resulting manuscript. This work has been supported by the projects PID2025-169859NB-I00 subsidised by Spanish Ministry of Science, Innovation and Universities. The research of FAF was funded by Programa Juan de la Cierva (ref. JDC2022-049170-I), financed by MCIU/AEI/10.13039/501100011033 and for the European Union NextGenerationEU/PRTR.

Editor: Andrzej Kaim

References

Alcock, A. 1900. Materials for a carcinological fauna of India, 5: The Brachyura Primigenia or Dromiacea. *Journal of the Asiatic Society of Bengal* 68 (II/3): 123–169.

Aurell, M. and Bádenas, B. 2015. Facies architecture of a microbial—siliceous sponge-dominated carbonate platform: the Bajocian of Moscardón (Middle Jurassic, Spain). *In*: D.W.J. Bosence, K.A. Gibbons, D.P. Le Heron, W.A. Morgan, T. Pritchard, and B.A. Vining (eds.), Microbial Carbonates in Space and Time: Implications for Global Exploration and Production. *Geological Society, London, Special Publications* 418: 155–174.

Aurell, M., Fregenal-Martínez, M., Bádenas, B., Muñoz-García, M.B., Élez, J., Meléndez, N., and de Santisteban, C. 2019. Middle Jurassic–Early Cretaceous tectono-sedimentary evolution of the southwestern Iberian Basin (central Spain): major palaeogeographical changes in the geotectonic framework of the Western Tethys. *Earth-Science Reviews* 199: 102983.

Aurell, M., Torromé, D., Gasca, J.M., Calvín, P., Pérez-Pueyo, M., Parrilla-Bel, J., Medrano-Aguado, E., Martín-Closas, C., Vicente, A., Sierra-Campos, P., and Canudo, J.I. 2022. Latest Cretaceous palaeogeographic evolution of northeast Iberia: Insights from the Campanian continental Montalbán subbasin (Spain). *Earth-Science Reviews* 235: 104251.

Aurell, M., Robles, S., Bádenas, B., Rosales, I., Quesada, S., Meléndez, G., and García-Ramos, J.C. 2003. Transgressive-regressive cycles and Jurassic palaeogeography of northeast Iberia. *Sedimentary Geology* 162 (3–4): 239–271.

Bádenas, B. and Aurell, M. 2018. The down-dip preferential sequence record of orbital cycles in greenhouse carbonate ramps: examples from the Jurassic of the Iberian Basin (NE Spain). *In*: M. Montenari (ed.), *Stratigraphy & Timescales, Cyclostratigraphy and Astrochronology. Vol.* 3, 285–325. Elsevier, Amsterdam.

Baucon, A., Avanzini, M., De Carvalho, C.N., Belaústegui, Z., Preto, N., and Breda, A. 2025. The earliest evidence of true crabs? Insights on the evolution of Brachyura from an exceptional exposure of Carnian *Psilonichnus* (Upper Triassic, Braies, Dolomites, Italy). *Palaeogeography, Palaeoclimatology, Palaeoecology* 667: 112820.

Blakey, R.C. 2021. *Deep Time Maps. Colorado Plateau Geosystems* (accessed September 2, 2026) [available online, https://deeptimemaps.com/].

Bersán, R. and Aurell, M. 1997. Origen y desarrollo de los montículos de esponjas y algas del Bajociense Superior de Ricla (Cordillera Ibérica Septentrional): *Cuadernos de Geología Ibérica* 22: 65–80.

Bulard, P.F. 1972. *Le Jurassique moyen et supérieur de la Chaine Ibérique sur la bordure du basin de l'Ebre*. 353 pp. Ph.D. Thesis, Nice University, Nice.

Collins, J.S.H. 1999. Fossils explained: Crab claws. *Geology Today* 15: 114–117.

Collins, J.S.H. and Wierzbowski, A. 1985. Crabs from the Oxfordian sponge megafacies of Poland. *Acta Geologica Polonica* 35: 73–88.

Crônier, C. and Boursicot, P.Y. 2009. A new decapod crustacean faunule from the Middle Jurassic of north-west France. *Palaeontology* 52: 1275–1289.

Davie, P.J., Guinot, D., and Ng, P.K.L. 2015. Phylogeny of Brachyura. *In*: P. Castro, P.J.F. Davie, D. Guinot, F.R. Schram, and J.C. Von Vaupel Klein (eds.), Decapoda: Brachyura (Part 2). *Treatise on Zoology—Anatomy, Taxonomy, Biology. The Crustacea, Vol. 9 Part C* (2 vols), 921–979. Brill, Leiden.

De Haan, W. 1833–1850. Crustacea. *In*: P.F. von Siebold (ed.), *Fauna Japonica sive descriptio animalium, quae in Itinere per Japoniam, Jussu et auspiciis superiorum, qui Summun in India Batava Imperium tenent, suscepto, annis 1823–1830 collegit, notis, observationibus et adumbrationibus illustravit*, i–xvii, i–xxxi, ix–xvi, 1–243. Ludguni Batavorum, Leiden.

Dupraz, C. and Strasser, A. 2002. Nutritional modes in coral-microbialite reefs (Jurassic, Oxfordian, Switzerland): evolution of trophic structure as a response to environmental change. *Palaios* 17: 449–471.

Étallon, A. 1861. Notes sur les Crustacés Jurassiques du bassin du Jura. *Mémoires de la Societé de l'Agriculture, des Sciences et Lettres de la Haute Saône* 9: 129–171.

Eudes-Deslongchamps, E. 1835. Mémoire sur les Teudopsides, animaux fossiles, voisins des calmars. *Mémoires de la Société Linnéenne de Normandie* 5: 68–78.

Eudes-Deslongchamps, E. 1877. *Le Jura Norman*. 60 pp. F. Savy, Paris.

Feldmann, R.M. and Schweitzer, C.E. 2010. Is *Eocarcinus* Withers, 1932, a basal brachyuran? *Journal of Crustacean Biology* 30: 241–250.

Feldmann, R.M., Lazăr, I., and Schweitzer, C.E. 2006. New crabs (Decapoda: Brachyura: Prosopidae) from Jurassic (Oxfordian) sponge bioherms of Dobrogea, Romania. *Bulletin of the Mizunami Fossil Museum* 33: 1–20.

Fernández-López, S.R. 1985. *El Bajociense en la Cordillera Iberica*. 850 pp. Ph.D. Thesis, Departamento de Paleontologia, Universidad Complutense de Madrid, Madrid.

Förster, R. 1979. *Eocarcinus praecursor* Withers (Decapoda, Brachyura) from the Lower Pliensbachian of Yorkshire and the early crabs. *Neues Jahrbuch für Geologie und Paläontologie, Monatshefte* 1979 (1): 15–27.

Förster, R. 1986. Der erste Nachweis eines brachyuren Krebses aus dem Lias (oberes Pliensbach) Mitteleuropas. *Mitteilungen der Bayerischen Staatssammlung für Paläontologie und historische Geologie* 26: 25–31.

Fraaije, R.H.B., Van Bakel, B.W.M., Guinot, D., and Jagt, J.W.M. 2013. A new Middle Jurassic (Bajocian) homolodromioid crab from northwest France; the earliest record of the Tanidromitidae. *Boletín de la Sociedad Geológica Mexicana* 65: 249–254.

Friebe, A. 1995. Die Schwammfazies im Mitteljura des nordöstlichen Keltiberikums (España). *Perfil* 8: 239–279.

Garassino, A. and Krobicki, M. 2002. *Galicia marianae* n. gen., n. sp. (Crustacea, Decapoda, Astacidea) from the Oxfordian (Upper Jurassic) of the southern Polish uplands. *Bulletin of the Mizunami Fossil Museum* 29: 51–59.

Gómez, J.J. and Fernández-López, S.R. 2006. The Iberian Middle Jurassic carbonate-platform system: Synthesis of the palaeogeographic elements of its eastern margin (Spain). *Palaeogeography, Palaeoclimatology, Palaeoecology* 236: 190–205.

Haug, J.T. and Haug, C. 2014. *Eoprosopon klugi* (Brachyura)—the oldest unequivocal and most "primitive" crab reconsidered. *Palaeodiversity* 7: 149–158.

Hée, A. 1924. Catalogue critique des Crustacés jurassiques du Calvados et de l'Orne. *Bulletin de la Société linnéenne de Normandie* 7 (6): 126–157.

Hyžný, M., Schlögl, J., and Krobicki, M. 2011. *Tanidromites insignis* (von Meyer, 1857) (Crustacea: Decapoda: Brachyura) from Late Jurassic non-biohermal facies of the Western Tethys (Pieniny Klippen Belt, Western Carpathians, Slovakia). *Neues Jahrbuch für Geologie und Paläontologie, Abhandlungen* 262: 213–226.

Hyžný, M., Starzyk, N., Robin, C.M., and Kočová-Veselská, M. 2015. Taxonomy and palaeoecology of a decapod crustacean assemblage from the Oxfordian of Stránská skála (Southern Moravia, Czech Republic). *Bulletin of Geosciences* 90: 633–650.

Jagt, J.W.M., Van Bakel, B.W.M., Guinot, D., Fraaije, R.H.B, and Artal, P. 2015. Fossil Brachyura. *In*: P. Castro, P.J.F. Davie, D. Guinot, F.R. Schram, and J.C. Von Vaupel Klein (eds.), Decapoda: Brachyura (Part 2). *Treatise on Zoology—Anatomy, Taxonomy, Biology. The Crustacea, Vol. 9 Part C* (2 vols), 847–920. Brill, Leiden.

Klompmaker, A.A., Hyžný, M., Portell, R.W., Jauvion, C., Charbonnier, S., Fussell, S.S., Klier, A.T., Tejera, R., and Jakobsen, S.L. 2019. Muscles and muscle scars in fossil malacostracan crustaceans. *Earth-Science Reviews* 194: 306–326.

Klompmaker, A.A., Starzyk, N., Fraaije, R.H.B., and Schweigert, G. 2020. Systematics and convergent evolution of multiple reef-associated Jurassic and Cretaceous crabs (Decapoda, Brachyura). *Palaeontologia Electronica* 23 (2): a32.

Krobicki, M. and Zatoń, M. 2008. Middle and Late Jurassic roots of brachyuran crabs: palaeoenvironmental distribution during their early evolution. *Palaeogeography, Palaeoclimatology, Palaeoecology* 263: 30–43.

Krobicki, M. and Zatoń, M. 2016. A new homolodromioid crab (Brachyura: Dromiacea: Tanidromitidae) from the Bajocian of central Poland and a review of the stratigraphical distribution and paleoenvironments of the known Middle Jurassic homolodromioids. *Journal of Crustacean Biology* 36: 695–715.

Latreille, P.A. 1802–1803. *Histoire naturelle, générale et particuliére, des Crustacés et des Insects, vol 3*. 468 pp. F. Dufart, Paris.

Leinfelder, R.R. and Schmid, D.U. 2000. Mesozoic reefal thrombolites and other microbolites. *In:* R.E. Riding and S.M. Awramik (eds.), *Microbial Sediments*, 289–294. Springer-Verlag, Berlin.

Leinfelder, R.R., Nose, M., Schmid, D.U., and Werner, W. 1993. Microbial crusts of the Late Jurassic: composition, palaeoecological significance and importance in reef construction. *Facies* 29: 195–229.

Leinfelder, R.R., Schmid, D.U., Nose, M., and Werner, W. 2002. Jurassic reef patterns; the expression of a changing globe. *In*: W. Kiessling, E. Flügel, and J. Golonka (eds.), *Phanerozoic Reef Patterns*, 465–520. Society for Sedimentary Geology (SEPM), Tulsa.

Martín-Chivelet, J., López-Gómez, J., Aguado, R., Arias, C., Arribas, J., Arribas, M.E., Aurell, M., Bádenas, B., Benito, M.I., Bover-Arnal, T., Casas-Sainz, A., Castro, J.M., Coruña, F., de Gea, G.A., Fornós, J.J., Fregenal-Martínez, M., García-Senz, J., Garófano, D., Gelabert, B., Giménez, J., González-Acebrón, L., Guimerà, J., Liesa, C.L., mas, R., Meléndez, N., Molina, J.M., Muñoz, J.A., Navarrete, R., Nebot, M., Nieto, L.M., Omodeo-Salé, S., Pedrera, A., Peropadre, C., Quijada, I.E., Quijano, M.L., Reolid, M., Robador, A., Rodríguez-López, J.P., Rodríguez-Perea, A., Rosales, I., Ruiz-Ortiz, P.A., Sàbat, F., Salas, R., Soria, A.R., Suarez-Gonzalez, P., and Vilas, L. 2019. The Late Jurassic–Early Cretaceous rifting. *In*: C. Quesada and J.T. Oliveira (eds.), J. Vergés and J.C. Kullberg (coord.), *The Geology of Iberia: A Geodynamic Approach. The Alpine Cycle*, 81. Springer, Cham.

Müller, P., Krobicki, M., and Wehner, G. 2000. Jurassic and Cretaceous primitive crabs of the family Prosopidae (Decapoda: Brachyura)—their taxonomy, ecology and biogeography. *Annales Societatis Geologorum Poloniae* 70: 49–79.

Ogg, J.G., Ogg, G.M., and Gradstein, F. 2016. *A Concise Geologic Time Scale: 2016*. 234 pp. Elsevier, Amsterdam.

Olivier, N., Lathuilière, B., and Thiry-Bastien, P. 2006. Growth models of Bajocian coral-microbialite reefs of Chargey-lès-Port (eastern France): palaeoenvironmental interpretations. *Facies* 52: 113–127.

Olivier, N., Pittet, B., Werner, W., Hantzpergue, P., and Gaillard, C. 2008. Facies distribution and coral-microbialite reef development on a low-energy carbonate ramp (Chay Peninsula, Kimmeridgian, western France). S*edimentary Geology* 205: 14–33.

Ossó, A., Van Bakel, B.W.M, and Ferratges, F.A. 2021. *Cuchiadromites jadeae*, a new genus and species of primitive crab (Crustacea: Decapoda: Podotremata) from the Aptian of Cantabria (Spain), with comments on its peculiar surface ornament. *Cretaceous Research* 117: 104636.

Ossó, À., van Bakel, B.W.M., Artal, P., Moreno-Bedmar, J.A., Sánchez-Beristain, F., and Bover-Arnal, T. 2023. An Aptian sponge-associated decapod crustacean assemblage from Cal Cassanyes (Catalonia, northeast Iberian Peninsula): Taxonomy and palaeoecological implications. *Cretaceous Research* 154: 105750.

Patrulius, D. 1959. Contributions à la systématique des décapodes néojurassiques. *Revue de Géologie et de Géographie* 3: 249–257.

Quenstedt, F.A. 1856–1858. *Der Jura*. 842 pp. Laupp, Tübingen.

Robin, N., Van Bakel, B.W.M., D'Hondt, J.L., and Charbonnier, S. 2015. A new early brachyuran (Crustacea, Decapoda) from the Middle Jurassic of northwest France, epibionts and ecological considerations. *Contributions to Zoology* 84 (3): 179–191.

Scholtz, G. 2020. *Eocarcinus praecursor* Withers, 1932 (Malacostraca, Decapoda, Meiura) is a stem group brachyuran. *Arthropod Structure & Development* 59: 100991.

Schweigert, G. and Koppka, J. 2011. Decapods (Crustacea: Brachyura) from the Jurassic of Germany and Lithuania, with descriptions of new species of *Planoprosopon* and *Tanidromites*. *Neues Jahrbuch für Geologie und Paläontologie, Abhandlungen* 260: 221.

Schweigert, G., Seegis, D.B., Fels, A., and Leinfelder, R.R. 1997. New internally structured decapod microcoprolites from Germany (late Triassic/early Miocene), southern Spain (early/Middle Jurassic) and Portugal (late Jurassic): taxonomy, palaeoecology and evolutionary implications. *Paläontologische Zeitschrift* 71: 51–69.

Schweitzer, C.E. and Feldmann, R.M. 2008. A new classification for some Jurassic Brachyura (Crustacea: Decapoda: Brachyura: Homolodromioidea): families Goniodromitidae Beurlen, 1932 and Tanidromitidae new family. *Senckenbergiana lethaea* 87 (for 2007): 119–156.

Schweitzer, C.E. and Feldmann, R.M. 2009a. New species of Longodromitidae Schweitzer and Feldmann, 2009, from the Ernstbrunn Formation, Late Jurassic (Tithonian), Austria. *Annalen des Naturhistorischen Museums Wien, Serie A* 111: 207–224.

Schweitzer, C.E. and Feldmann, R.M. 2009b. Revision of *Gabriella* Collins et al., 2006 (Decapoda: Brachyura: Homolodromioidea: Tanidromitidae) with new Jurassic species. *Neues Jahrbuch für Geologie und Paläontologie, Abhandlungen* 252: 1–16.

Schweitzer, C.E. and Feldmann, R.M. 2009b. Revision of the Prosopinae sensu Glaessner, 1969 (Crustacea: Decapoda: Brachyura) including four new families, four new genera, and five new species. *Annalen des Naturhistorischen Museums in Wien*, *Serie A* 110: 55–121.

Schweitzer, C.E. and Feldmann, R.M. 2011. Revision of some fossil podotrematous Brachyura (homolodromiidae; Longodromitidae; Torynommidae). *Neues Jahrbuch fur Geologie und Palaontologie, Abhandlungen* 260: 237.

Schweitzer, C.E., Feldmann, R.M., and Lazăr, I.R. 2007. Decapods from Jurassic (Oxfordian) sponge megafacies of Dobrogea, Romania and reconsideration of *Nodoprosopon* Beurlen, 1928. *Neues Jahrbuch für Geologie und Paläontologie, Abhandlungen* 244: 99–113.

Schweitzer, C.E., Feldmann, R.M., Lazăr, I., Schweigert, G., and Franţescu, O.D. 2018. Decapoda (Anomura; Brachyura) from the Late Jurassic of the Carpathians, Romania; *Neues Jahrbuch für Geologie und Paläontologie, Abhandlungen* 288: 307–341.

Schweitzer, C.E. Feldmann, R.M., Rader, W.L., and Franţescu, O. 2016. Early Cretaceous (Albian) decapods from the Glen Rose and Walnut formations of Texas, USA. *Bulletin of the Mizunami Fossil Museum* 42: 1–22.

Starzyk, N. 2013. Jurassic crabs: new characters of carapace diagnostic to known tanidromitid species. *Neues Jahrbuch für Geologie und Paläontologie, Abhandlungen* 269: 173–187.

Starzyk, N. 2015. Reappraisal of the primitive crab *Eodromites*, with description of three new species from European localities (Decapoda: Brachyura: Goniodromitidae). *Palaeontologia Electronica* 18 (3): 1–19.

Starzyk, N. 2016. Three new species of the genus *Tanidromites* (Decapoda: Brachyura: Tanidromitidae) from the late Jurassic (Oxfordian) of Poland. *Palaeontologia Electronica* 19.3.45A: 1–14.

Tomás, S., Aurell, M., Bádenas, B., Bjorge, M., Duaso, M., and Mutti,

M. 2019. Architecture and paleoenvironment of Mid-Jurassic microbial-siliceous sponge mounds, northeastern Spain. *Journal of Sedimentary Research* 89: 110–134.

Tsang, L.M., Schubart, C.D., Ahyong, S.T., Lai, J.C.Y., Au, E.Y.C., Chan, T.Y., Ng, P.K.L., and Chu, K.H. 2014. Evolutionary history of true crabs (Crustacea: Decapoda: Brachyura) and the origin of freshwater crabs. *Molecular Biology and Evolution* 31: 1173–1187.

Van Bakel, B.W.M. and Guinot, D. 2023. New genera and species of glaessneropsid crabs from the Lower and Middle Jurassic of France and Germany-Austria, and reconsolidation of *Charassocarcinus* Van Straelen, 1925. *Geobios* 79: 61–76.

Van Bakel, B.W.M, Maerten, L., Jagt, J.W.M., and Fraaije, R.H.B. 2021. *Bajoprosopon piardi* n. gen. and sp. from the Middle Jurassic of France, with a revised diagnosis of the family Prosopidae von Meyer, 1860 (Brachyura, Podotremata) and notes on the availability of names introduced by Hermann von Meyer (1835, 1857). *Palaeontologia Electronica*: art. 24.2.a26.

Van Straelen, V. 1925. Contribution à l'étude des crustacés décapodes de la période Jurassique. *Mémoires de l'Académie royale de Belgique, Classe des Sciences* 7(2): 1–462.

Via, L. and Sequeiros, L. 1989. Cangrejos máscara (Prosopidae) del Oxfordiense de Moneva (Zaragoza). *Batalleria* 3: 5–16.

Von Meyer, H. 1840. *Neue Gattungen fossiler Krebse aus Gebilden vom Bunten Sandstein bis in die Kreide.* 28 pp. Schweizerbart, Stuttgart.

Von Meyer, H. 1842. Ueber die in dem dichten gelben Jurakalk von Aalen in Würtemberg vorkommenden Species des Crustaceengenus *Prosopon*. *Beiträge zur Petrefacten-Kunde* 5: 70–75.

Von Meyer, H. 1857. Briefliche Mittheilungen. *Neues Jahrbuch für Mineralogie, Geologie, Geognosie und Petrefakten-Kunde* 1857: 556.

Von Meyer, H. 1860. Die Prosoponiden oder die Familie der Maskenkrebse. *Palaeontographica* 7: 183–222.

Wehner, G. 1988. *Über die Prosoponiden (Crustacea, Decapoda) des Jura*. 154 pp. Dissertation zur Erlangung des Doktorgrades der Fakultät für Geowissenschaften der Ludwig-Maximilians-Universität zu München, Munich.

Withers, T.H. 1932. A Liassic crab, and the origin of the Brachyura. *The Annals and Magazine of Natural History* 10: 313–323.

Wolfe, J.M., Breinholt, J.W., Crandall, K.A., Lemmon, A.R., Lemmon, E.M., Timm, L.E., Siddall, M.E., and Bracken-Grissom, H.D. 2019. A phylogenomic framework, evolutionary timeline and genomic resources for comparative studies of decapod crustaceans. *Proceedings of the Royal Society B* 286 (1901): 20190079.

Wolfe, J.M., Luque, J., and Bracken-Grissom, H.D. 2021. How to become a crab: Phenotypic constraints on a recurring body plan. *BioEssays* 43 (5): 2100020.

Woodward, H. 1907. On a new brachyurous Crustacean from the "Clypeus-Grit" (Inf. Oolite) of the Cotteswold Hills. *Geological Magazine, new series* 4: 79–81.